The EMBO Journal (2006) 25, 4524–4536 | © 2006 European Molecular Biology Organization | All Rights Reserved 0261-4189/06
www.embojournal.org

THE EMBO JOURNAL

A novel proteasome interacting protein recruits the deubiquitinating enzyme UCH37 to 26S proteasomes

Jun Hamazaki[1,2], Shun-ichiro Iemura[3], Tohru Natsume[3], Hideki Yashiroda[1], Keiji Tanaka[1] and Shigeo Murata[1,4,*]

[1]Laboratory of Frontier Science, Core Technology and Research Center, Tokyo Metropolitan Institute of Medical Science, Bunkyko-ku, Tokyo, Japan, [2]Department of Biological Sciences, Graduate School of Science, Tokyo Metropolitan University, Hachiohji, Tokyo, Japan, [3]National Institutes of Advanced Industrial Science and Technology, Biological Information Research Center, Kohtoh-ku, Tokyo, Japan and [4]PRESTO, Japan Science and Technology Agency, Kawaguchi, Saitama, Japan

The 26S proteasome is a multisubunit protease responsible for regulated proteolysis in eukaryotic cells. It is composed of one catalytic 20S proteasome and two 19S regulatory particles attached on both ends of 20S proteasomes. Here, we describe the identification of Adrm1 as a novel proteasome interacting protein in mammalian cells. Although the overall sequence of Adrm1 has weak homology with the yeast Rpn13, the amino- and carboxyl-terminal regions exhibit significant homology. Therefore, we designated it as hRpn13. hRpn13 interacts with a base subunit Rpn2 via its amino-terminus. The majority of 26S proteasomes contain hRpn13, but a portion of them does not, indicating that hRpn13 is not an integral subunit. Intriguingly, we found that hRpn13 recruits UCH37, a deubiquitinating enzyme known to associate with 26 proteasomes. The carboxyl-terminal regions containing KEKE motifs of both hRpn13 and UCH37 are involved in their physical interaction. Knockdown of hRpn13 caused no obvious proteolytic defect but loss of UCH37 proteins and decrease in deubiquitinating activity of 26S proteasomes. Our results indicate that hRpn13 is essential for the activity of UCH37.

The EMBO Journal (2006) **25,** 4524–4536. doi:10.1038/sj.emboj.7601338; Published online 21 September 2006
Subject Categories: proteins
Keywords: deubiquitinating enzyme; proteasome; Rpn13; ubiquitin; UCH37

Introduction

The ubiquitin–proteasome system is the main non-lysosomal route for intracellular protein degradation in eukaryotes (Glickman and Ciechanover, 2002). Short-lived proteins as well as abnormal proteins in cells are recognized by the ubiquitin system and are marked with ubiquitin chains as a degradation signal. Polyubiquitinated proteins are then recognized and degraded by 26S proteasomes. The 26S proteasome is a huge protein complex of approximately 2.5 MDa composed of one proteolytically active 20S proteasome and two 19S regulatory particles (RP), each attached to one end of the 20S proteasome (Baumeister *et al*, 1998). The 20S proteasome is a barrel-shaped complex formed by the axial stacking of four rings made up of two outer α-rings and two inner β-rings, which are each made up of seven structurally similar α- and β-subunits, respectively, being associated in the order of $\alpha_{1-7}\beta_{1-7}\beta_{1-7}\alpha_{1-7}$ (Coux *et al*, 1996). The interior of the cavity composed of β-rings is responsible for its proteolytic activity. However, the entry of substrates into the cavity of 20S proteasomes is restricted by the narrow gate of α-rings, which is closed in itself. The 19S RP plays an important role in the degradation of ubiquitinated proteins. The 19S RP can be divided into two subcomplexes, known as 'base' and 'lid' (Glickman *et al*, 1998). The base is made up of six ATPases (Rpt1–Rpt6) and two large regulatory components, Rpn1 and Rpn2, functioning as presumptive receptor(s) of ubiquitin-like proteins (Leggett *et al*, 2002), whereas the lid contains multiple non-ATPase subunits (Rpn3, Rpn5–9, Rpn11–13, and Rpn15). The base complex binds to the outer α-ring of the 20S proteasome and opens a narrow gate in an ATP-dependent manner (Smith *et al*, 2005). In addition, the ATPase subunits supply energy for unfolding target proteins, so that they can be translocated into the β-ring cavity of 20S proteasomes where active sites are located. The role of the lid complex is less unraveled. Among the lid subunits, Rpn11 is known as a metalloprotease that cleaves the peptide bonds between the substrate and the most proximal ubiquitin of the polyubiquitin chains (Verma *et al*, 2002; Yao and Cohen, 2002). Rpn10 is thought to lie between the base and the lid complex and serve as one of the ubiquitin receptors (Verma *et al*, 2004).

In addition to the genuine proteasome subunits, several molecules that associate with proteasomes and play auxiliary roles have been identified (Verma *et al*, 2000; Leggett *et al*, 2002). Most of the proteasome studies have been carried out using yeast cells, especially budding yeasts, and less is known about mammalian proteasomes and some of the counterparts of yeast proteasome subunits have not yet been identified. Here, we show that Adrm1, which was previously reported as a membrane glycoprotein (Shimada *et al*, 1991, 1994), is an ortholog of yeast Rpn13 and identify it as a novel interacting protein of mammalian 26S proteasomes. Furthermore, we reveal that it recruits UCH37, a deubiquitinating enzyme (DUB) associated with proteasomes (Lam *et al*, 1997; Li *et al*, 2000; Stone *et al*, 2004).

Results

Adrm1 is a mammalian ortholog of yeast Rpn13

To identify proteins involved with mammalian proteasomes, we searched for cellular proteins that physically associate,

*Corresponding author. Laboratory of Frontier Science, Core Technology and Research Center, Tokyo Metropolitan Institute of Medical Science, 3-18-22 Honkomagome, Bunkyko-ku, Tokyo 113-9613, Japan. Tel./Fax: +81 3 3823 2237; E-mail: smurata@rinshoken.or.jp

Received: 21 February 2006; accepted: 15 August 2006; published online: 21 September 2006

directly or indirectly, with 26S proteasomes in mammalian cells. For this purpose, the human ortholog of Rpn10 (hRpn10: hereafter, 'h' is used as a prefix to indicate a human ortholog of any yeast proteasome subunit) with a carboxyl-terminal Flag tag was expressed in HEK293 cells and immunoprecipitated from cell lysates with anti-Flag antibody. The immunoprecipitates were eluted with Flag peptides, digested with Lys-C endopeptidase, and analyzed using a highly sensitive direct nano-flow liquid chromatography/tandem mass spectrometry (LC–MS/MS) (Natsume *et al*, 2002). Following a database search, 30 peptides were assigned to MS/MS spectra for Flag-hRpn10-associated complexes (Supplementary Figure 1). These data identified almost all the subunits of 26S proteasomes. In addition, we identified a molecule with yet unknown relevance to proteasomes, called Adrm1.

Adrm1 was previously reported as a membrane glycoprotein with a molecular mass of 110 kDa and involved in cell adhesion (Shimada *et al*, 1994; Simins *et al*, 1999; Natsume *et al*, 2002). Exploration of the Proteome BioKnowledge Library (https://www.proteome.com/proteome/Retriever/index.html) database indicated that Adrm1 is weakly homologous to Rpn13, a subunit of budding yeast proteasomes (Verma *et al*, 2000). The overall sequence of Adrm1 showed 24.9% homology with that of Rpn13, whereas it exhibited a high homology of 60.2% with the amino-termini of Adrm1 (residues 22–111) and Rpn13 (residues 7–103). We also identified 74.4% homology between the C-termini of Adrm1 (residues 366–407) and Rpn13 (residues 114–156) (Figure 1). Accordingly, we renamed the molecule hRpn13.

Identification of hRpn13 as a novel proteasome interacting protein in mammals

To verify that hRpn13 is a human counterpart of yeast Rpn13, we tested whether hRpn13 is incorporated into 26S proteasomes. Extracts of 293T cells were fractionated by glycerol gradient centrifugation, and each fraction was subjected to immunoblotting with anti-hRpn13 antibody. Almost all hRpn13 proteins co-sedimented with 26S proteasomes that were detected by succinyl-Leu-Leu-Val-Tyr-7-amido-4-methylcoumarin (Suc-LLVY-MCA)-hydrolyzing activity and sedimentation of a genuine proteasome subunit hRpn1 (Figure 2A). Free forms of hRpn13 were not apparently observed (Figure 2A). 26S proteasomes were further purified from fractions 18–20 by immunoprecipitation using anti-hRpt6 antibody, and then the immunoprecipitates were subjected to two-dimensional polyacrylamide gel electrophoresis (2D-PAGE). Immunoblot for hRpn13 detected a spot that had an isoelectric point (p*I*) and molecular mass that corresponded to the predicted values of p*I* 4.8 and 42.1 kDa, respectively (Figure 2B). Tandem mass spectrometric analysis identified this spot as Adrm1 (data not shown). Adrm1 has been reported as a glycosylated membrane protein with a molecular mass of 110 kDa (Shimada *et al*, 1994), which is in conflict with the notion that Adrm1, that is, hRpn13, is a subunit of proteasomes. Immunostaining of HeLa cells using anti-hRpn13 and anti-hRpn1 antibodies showed that the distribution of hRpn13 was mainly in the nucleus and partially in the cytosol, a pattern quite similar to the distribution of hRpn1 (Figure 2C). These results were in agreement with those reported previously showing that proteasomes are predominantly present in the nuclei of rapidly proliferating mammalian cells (Kumatori *et al*, 1990). Thus, in our hands, there was no evidence that hRpn13 is a membrane protein.

Next, we examined whether all 26S proteasomes contain hRpn13. The 26S proteasome fractions (fractions 18–20 in Figure 2A) were immunodepleted using anti-hRpt6 antibody, anti-hRpn13 antibody, or preimmune serum. Anti-hRpt6 antibody completely immunodepleted hRpn13 and other 19S RP

Figure 1 Sequence alignment of human Adrm1 and budding yeast Rpn13. The amino-acid sequences were aligned by the DIALIGN-T program. Amino acids that are identical, strongly similar, and weakly similar between the two sequences are boxed in black, dark gray, and light gray, respectively. Hs: *Homo sapiens*; Sc: *Saccharomyces cerevisiae*.

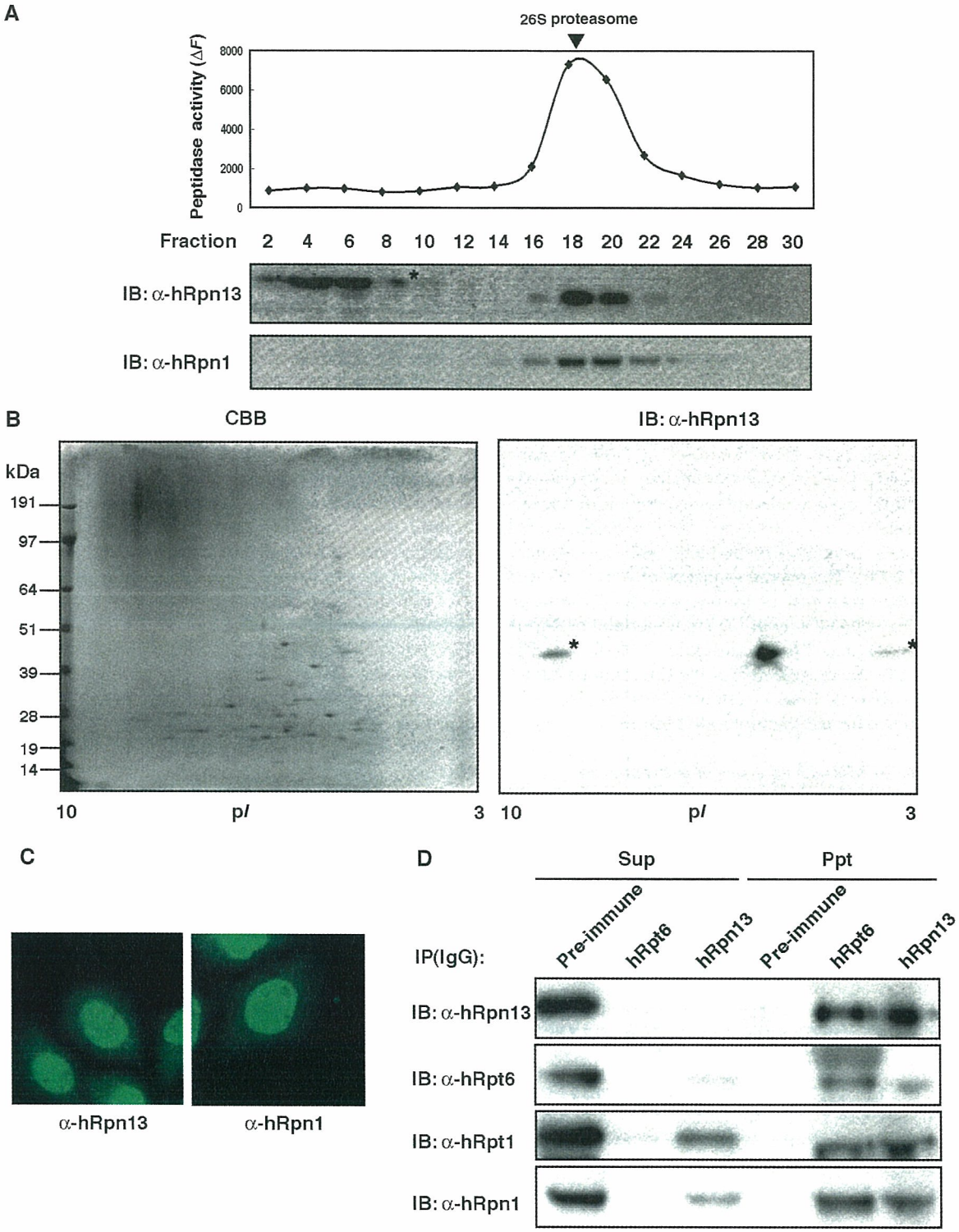

Figure 2 hRpn13 is a subunit of mammalian 26S proteasomes. (**A**) Sedimentation velocity analysis. Extracts of HEK293T cells were fractionated by 10–40% glycerol gradient centrifugation into 32 fractions from the top. An aliquot of each fraction was subjected to the assay of Suc-LLVY-MCA-hydrolyzing activity (upper panel). Immunoblot analysis of each fraction was performed using antibodies against hRpn1 and hRpn13 (lower panels). Arrowhead indicates the peak fraction of 26S proteasomes. Asterisk indicates artifact bands. (**B**) Affinity purification of human proteasomes. Fractions 18–20 in panel A were subjected to immunoprecipitation using anti-hRpt6 antibody. The precipitates were eluted with glycine–HCl and resolved by 2D-PAGE, followed by Coomassie brilliant blue (CBB) staining (left panel) and immunoblot with anti-hRpn13 antibody (right panel). (**C**) Intracellular distribution of hRpn13 in HeLa cells. hRpn13 (left panel) and hRpn1 (right panel) were detected with anti-hRpn13 or anti-hRpn1 antibody and visualized with Alexa488-conjugated anti-rabbit IgG antibody. (**D**) Immunodepletion analysis. Fractions 18–20 in panel A were pooled and immunoprecipitated with anti-hRpt6 antibody, anti-hRpn13 antibody, or preimmune serum. The unbound fractions and immunoprecipitates were subjected to SDS–PAGE, followed by immunoblotting for hRpn13, hRpt6, hRpt1, and hRpn1.

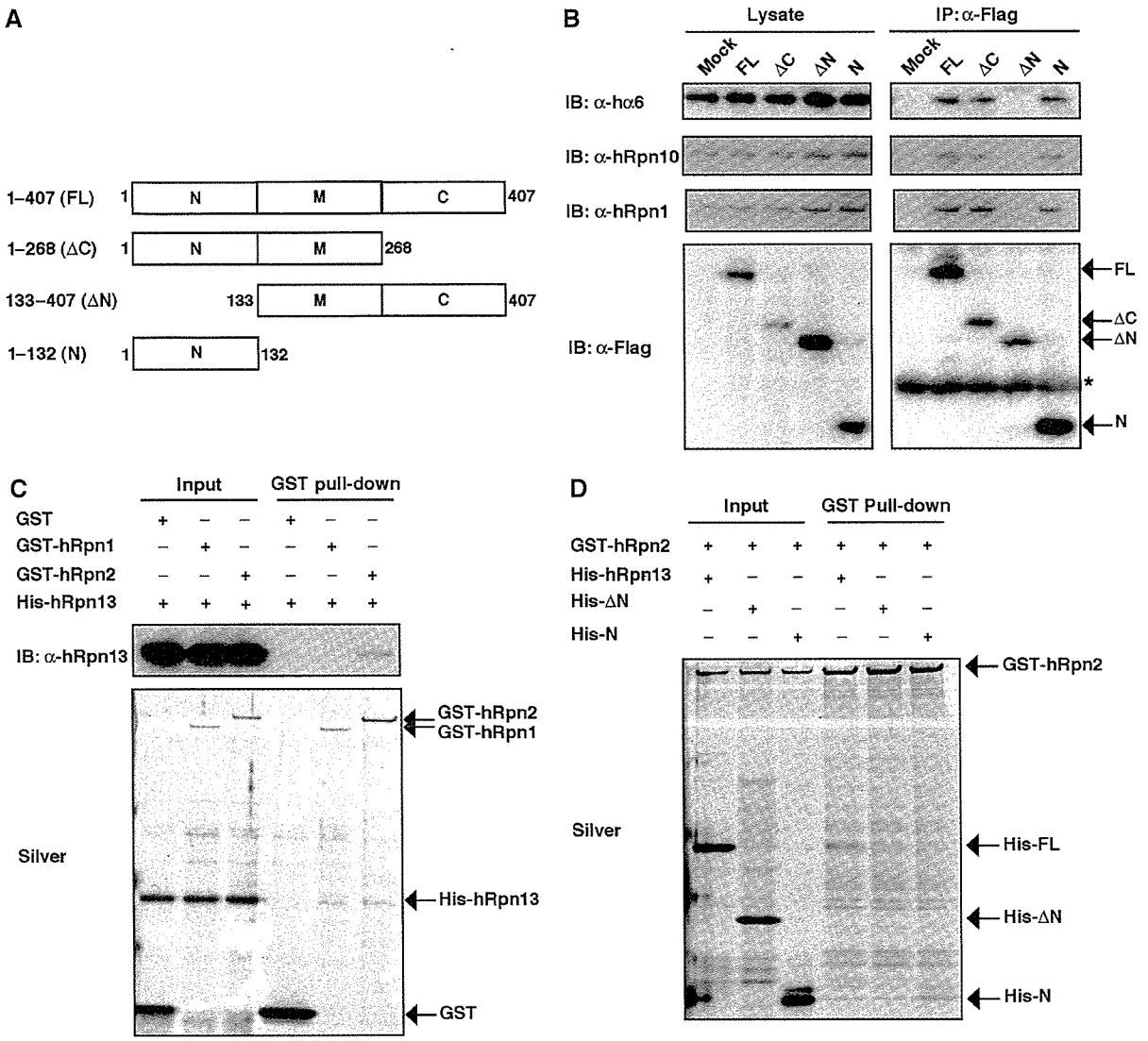

Figure 3 hRpn13 associates with proteasomes via its N-terminal region. (**A**) Schematic representation of constructs for Rpn13 and its dissected mutants used. (**B**) Flag-tagged plasmids encoding hRpn13 and its deletion mutants depicted in panel A were transfected into HEK293T cells. The cell lysates were immunoprecipitated with anti-Flag antibody, followed by immunoblotting for hα6, hRpn10, hRpn1, and Flag epitopes. (**C**) GST pull-down analysis of recombinant proteins. GST, GST-hRpn1, and GST-hRpn2 were incubated with 6xHis-hRpn13 for 1 h at 4°C and then precipitated with glutathione Sepharose. The bound proteins were analyzed by SDS–PAGE, followed by silver staining and immunoblotting with anti-hRpn13 antibody. (**D**) GST pull-down analysis of recombinant proteins. GST-hRpn2 was incubated with 6xHis-hRpn13 or its mutant forms and then pulled down with glutathione Sepharose followed by silver staining.

subunits such as hRpt1 and hRpn1. In contrast, anti-hRpn13 antibody did not remove all the 19S RP subunits, with about 10% input of 19S RP being left in the unbound fraction, whereas it completely depleted hRpn13 (Figure 2D). These results indicate that hRpn13 is incorporated into the majority of 26S proteasomes, but a portion of 26S proteasomes does not contain hRpn13. Therefore, we conclude that hRpn13 is one of the near-stoichiometric proteasome interacting proteins (PIPs), like Ubp6 and Ecm29 in budding yeast (Leggett *et al*, 2002), and is not an integral subunit of 26S proteasomes.

The conserved N-terminal region of hRpn13 is required for association with proteasomes

Based on the sequence alignment, we postulated that hRpn13 is composed of three regions. The N- and C-terminal regions are conserved between budding yeast and human, and the internal region that lies between the N- and C-terminal regions is not found in the budding yeast Rpn13 (Figure 1). We tentatively divided hRpn13 into three portions. The 'N' portion encompassed the conserved N-terminal region (i.e. amino acids 1–132) and the 'C' portion corresponded to amino acids 269–407 that included the conserved C-terminal region. The portion between 'N' and 'C' was designated 'M' portion (Figure 3A). In the next step, we determined the portion required for incorporation into proteasomes. Various deletion constructs encoding wild-type and mutant hRpn13 with Flag tag were expressed in HEK293T cells and immunoprecipitated with anti-Flag antibody. The hRpn13 mutants that lacked the C portion or encoded solely the N portion precipitated various proteasome subunits such as hα6, hRpn10, and hRpn1, as did full-length hRpn13 (Figure 3B). In contrast, hRpn13 that lacked the N portion did not precipitate these subunits (Figure 3B). These results indicate

that the N portion, that is, the conserved N-terminal region of hRpn13, is essential and sufficient for its association with proteasomes.

hRpn13 directly interacts with a base subunit hRpn2

The next set of experiments determined the subunit of 26S proteasomes associated with hRpn13. For this purpose, we tested the interaction between hRpn13 and each subunit of mammalian 19S RP by yeast two-hybrid analysis. The results identified hRpn1 and hRpn2 as possible interacting subunits with hRpn13 (data not shown). Furthermore, comprehensive interactive proteome analysis in budding yeast showed interaction of Rpn13 with Rpn2 (Ito *et al*, 2001). Therefore, we purified recombinant proteins of hRpn1, hRpn2, and hRpn13 and performed *in vitro* binding analysis (Figure 3C). hRpn13 was pulled down by glutathione *S*-transferase (GST)-hRpn2 but not by GST-hRpn1, indicating that hRpn13 is directly associated with hRpn2. Next, we tested whether the N-terminal region of hRpn13 is required for the association with hRpn2. As shown in Figure 3D, the N portion of hRpn13 was required and sufficient for interaction with GST-hRpn2, which was consistent with the results shown in Figure 3B. Based on these results, we conclude that hRpn13 is associated with 26S proteasomes via hRpn2, with which the conserved N-terminal region of hRpn13 interacts.

Knockdown of Rpn13 does not cause proteolytic defects in proteasomes

In budding yeast, deletion of Rpn13 is not lethal, unlike most other proteasome subunits, but causes defect in the degradation of a ubiquitin-fusion-degradation (UFD) substrate (Verma *et al*, 2000). To elucidate the function of hRpn13 in mammalian cells, we knocked down hRpn13 by small interfering RNA (siRNA) in HEK293T cells. As a positive control for proteasome dysfunction, knockdown of hRpt2 was also performed. In hRpt2 knockdown cells, a decrease in hRpt2 protein levels resulted in a concomitant loss of hRpn13 as well as other genuine proteasome subunits such as hRpn1 and hα6. Consequently, hRpt2-knockdown cells showed cell death (data not shown) and accumulation of polyubiquitinated proteins (Figure 4A), which are hallmarks of proteasome dysfunction. These results indicate that hRpt2 is required for the integrity of proteasome structure and function and that hRpn13 is stably expressed in the presence of normal proteasomes. In hRpn13-knockdown cells, the expression of hRpn13 was almost abrogated, but the expression of other proteasome subunits was not changed (Figure 4A). The cells showed normal growth (data not shown) and no accumulation of polyubiquitinated proteins (Figure 4A). These features were in contrast to the phenotypes of hRpt2 knockdown. When the extracts from HEK293T cells were fractionated by glycerol-density gradient centrifugation, an active enzyme that catalyzes the degradation of the fluorogenic substrate Suc-LLVY-AMC was sedimented with a sedimentation coefficient of approximately that of 26S, but low activity was found in the slowly sedimenting fractions corresponding to the sedimentation position of the purified 20S proteasome (Figure 4B, upper panel). The addition of 0.05% SDS, which is a potent artificial activator of the latent 20S proteasome, caused marked activation of the enzyme sedimenting like the 20S proteasome (Figure 4B, lower panel). As shown in Figure 4B, the peptide-hydrolyzing activities of both 20S and 26S proteasomes remained unchanged irrespective of hRpn13 knockdown. Next, we tested the activities of protein degradation *in vitro* (Figure 4C and D) and *in vivo* (Figure 4E). Assay of antizyme (AZ)-dependent ornithine decarboxylase (ODC) degradation, which measures ATP-dependent and ubiquitin-independent proteolytic activity of 26S proteasomes (Murakami *et al*, 1992), did not show decreased proteolytic activity. Rather, the activity was increased 1.4-fold in the hRpn13-knockdown cells (Figure 4C). We also examined ubiquitin-dependent proteolytic activity using *in vitro* ubiquitinated cIAP1 (inhibitor of apoptosis-1), which is a ubiquitin ligase that catalyzes its own ubiquitination for degradation (Yang *et al*, 2000). As shown in Figure 4D, extracts of hRpn13-knockdown cells showed normal proteolytic activity in the degradation of ubiquitinated cIAP1 proteins. IκBα is also a well-known substrate of 26S proteasomes that is rapidly ubiquitinated and degraded in response to TNF-α (Suzuki *et al*, 2000). To check proteasome activities *in vivo*, we monitored the degradation rate of IκBα. hRpn13-knockdown cells showed the same degradation efficiency as control cells (Figure 4E). Considered together, the above results suggest that hRpn13 is not essential for overall protein degradation and viability of mammalian cells.

hRpn13 interacts with UCH37 via its C-terminus

Whereas the N-terminal region of hRpn13 is essential for association with 26S proteasomes (Figure 3), the role of the conserved C-terminal region is still unknown. To elucidate its role, we again used the proteomic approach. Flag-tagged hRpn13ΔN that did not interact with proteasomes (Figure 3) was expressed in HEK293 cells and immunoprecipitated from the cell lysate with anti-Flag antibody, followed by LC–MS/MS analysis. The peptides most abundantly identified were those of UCH37 (also called UCHL5) (Figure 5A), which is reported to be associated with proteasomes in fission yeast, fly, and mammals (Lam *et al*, 1997; Holzl *et al*, 2000; Li *et al*, 2000, 2001; Stone *et al*, 2004). We noticed that both hRpn13 and UCH37 had KEKE motifs at their C-terminal extremities. The conserved C-terminal region of hRpn13 is composed of one typical KEKE at its C-terminus (hereafter referred to as KE2) and one KE-rich region adjacent to KE2, which does not fit the definition of KEKE motif, as proposed previously (Realini *et al*, 1994), but is rich in lysine and glutamic acid residues (hereafter referred to as KE1) (Figure 5B, left panel). A proline residue known as a potent α-helical and β-sheet structure breaker (MacArthur and Thornton, 1991) was located between KE1 and KE2. KEKE motifs are known to mediate protein–protein interactions (Realini *et al*, 1994), and we hypothesized that the interaction between these two molecules was KEKE motif dependent. To test this notion, we expressed Flag-tagged hRpn13, hRpn13ΔKE2 lacking typical KEKE motif, and hRpn13ΔKE1 + 2, which lacked both KE1 and KE2 and thus the entire conserved C-terminal region, in HEK293T cells and immunoprecipitation was achieved with anti-Flag antibody (Figure 5B, right panel). Although the three constructs precipitated nearly the same amount of hα6 and hRpn1, hRpn13ΔKE2 precipitated less amount of UCH37 compared with the wild-type hRpn13, and hRpn13ΔKE1 + 2 did not precipitate UCH37. These results indicate that the conserved C-terminal region is required for the interaction with UHC37.

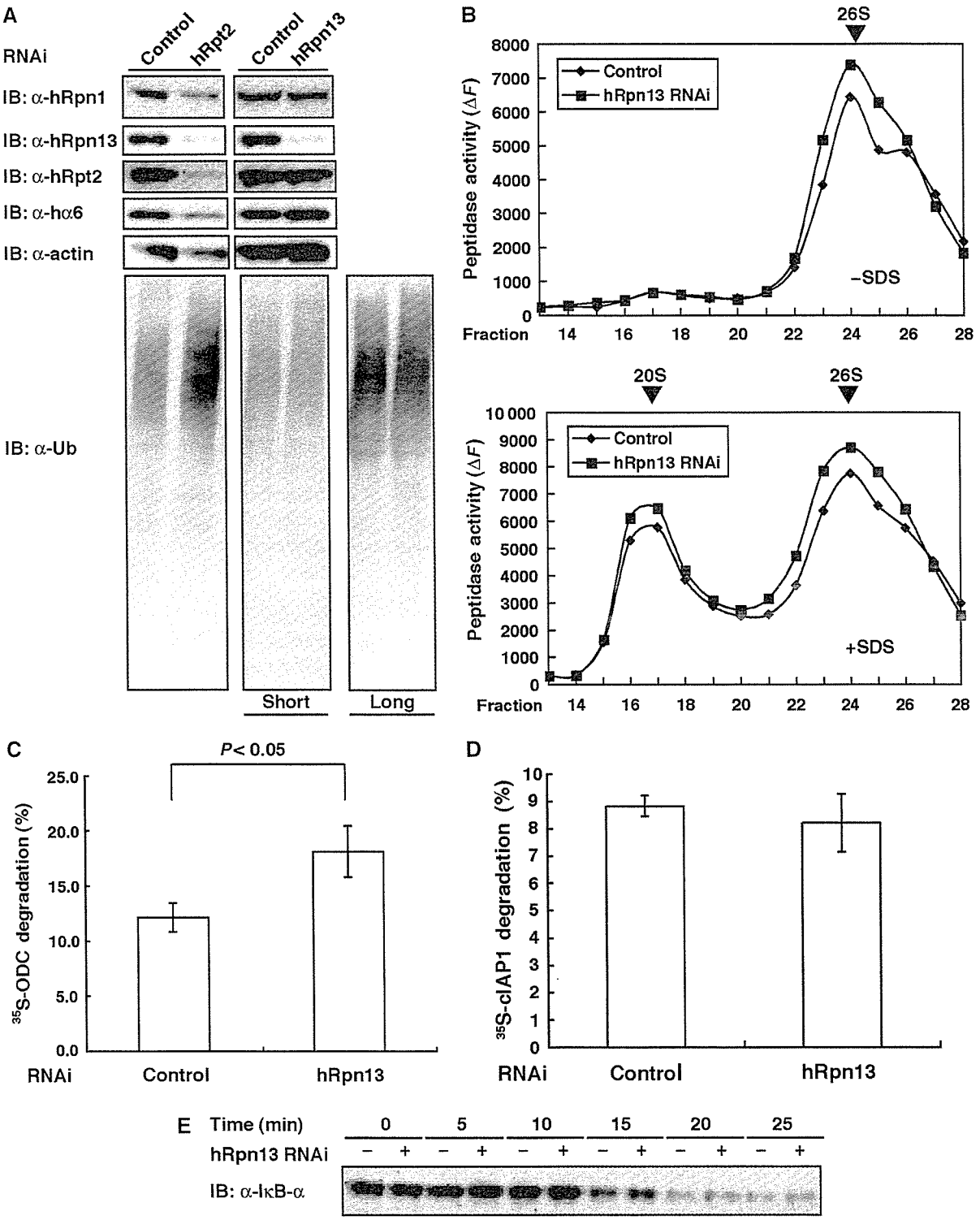

Figure 4 siRNA-mediated knockdown of hRpn13 does not cause proteolytic defects in proteasomes. (**A**) HEK293T cells were transfected with siRNA against hRpn13 or hRpt2. After 48 h for hRpt2 knockdown and 96 h for hRpn13 knockdown, cell extracts were subjected to SDS–PAGE, followed by immunoblotting with the indicated antibodies. (**B**) Extracts of control and Rpn13-knockdown cells were fractionated by 8–32% glycerol gradient centrifugation into 32 fractions from the top. Suc-LLVY-AMC hydrolysis activities were measured in the absence (left) or presence (right) of 0.05% SDS. 20S: 20S proteasome; 26S: 26S proteasome. (**C**) Ubiquitin-independent protein-degrading activity of proteasome. ATP- and AZ-dependent degradation of ^{35}S-labeled ODC protein was assayed. Knockdown cells showed significantly increased activity ($P<0.05$, one-way analysis of variance). Data are mean±s.e.m. values of three independent experiments. (**D**) Ubiquitinated cIAP1-degrading activity of proteasomes. Ubiquitin-dependent degradation of ubiquitinated ^{35}S-labeled cIAP1 was assayed. Data are mean±s.e.m. values of three independent experiments. (**E**) Effect of hRpn13 knockdown on TNF-α-induced degradation of IκBα *in vivo*. HEK293T cells were treated with TNF-α for the indicated times in the presence of cycloheximide. The levels of IκBα proteins were analyzed by immunoblotting.

A

Protein symbol	Protein name	Peptides
UCH37	Ubiquitin carboxy-terminal hydrolase 37	7
TIMM13	Translocase of inner mitochondrial membrane 13 homolog	4
YWHAE	14-3-3 epsilon	4
PRDX1	Peroxiredoxin 1	2
USMG5	Upregulated during skeletal muscle growth 5	2
BUB3	BUB3 budding uninhibited by benzimidazoles 3 homolog	1
TIMM8A	Translocase of inner mitochondrial membrane 8 homolog A	1

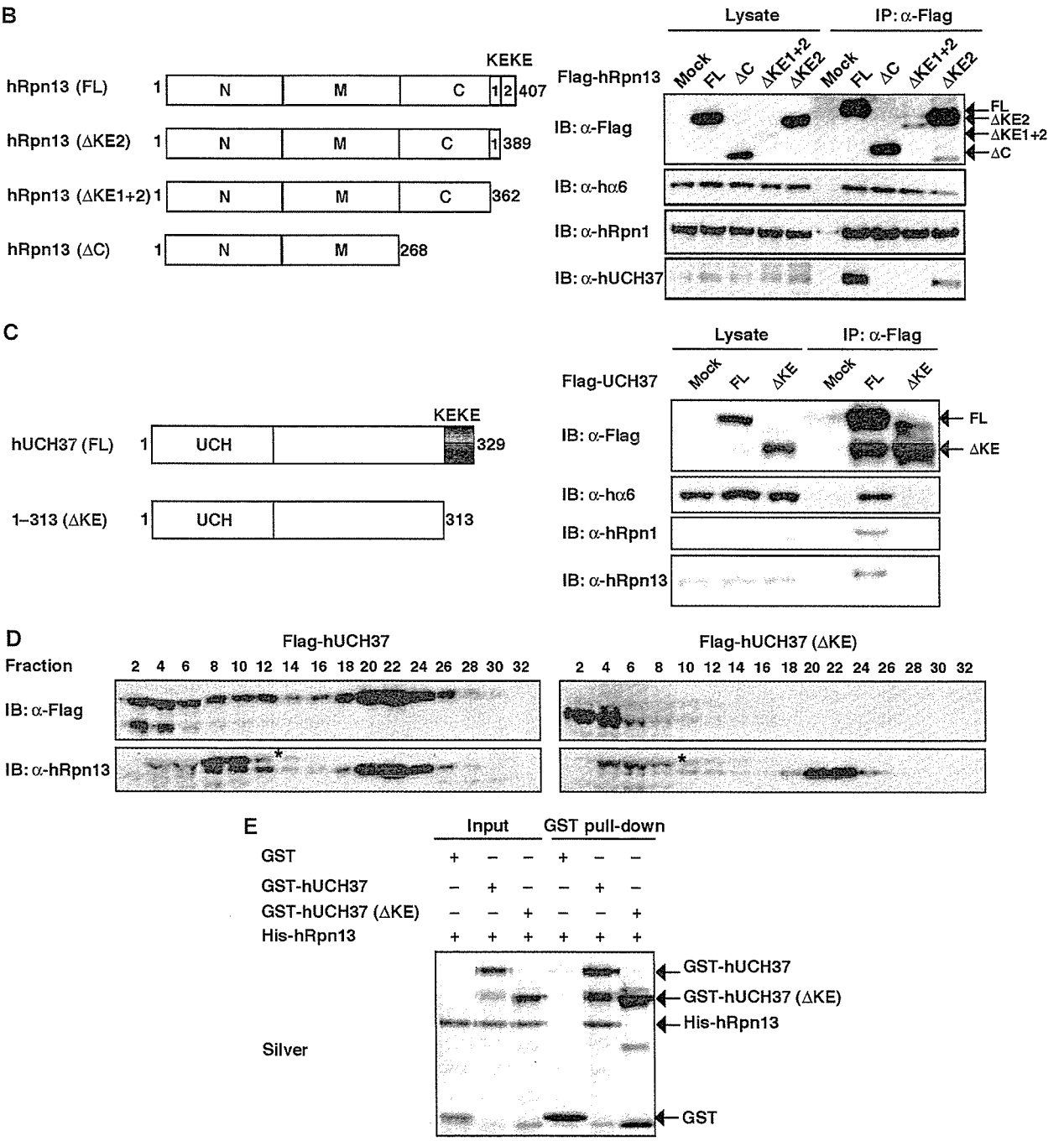

Figure 5 UCH37 interacts with hRpn13. (**A**) A list of proteins detected in four independent hRpn13ΔN immunoprecipitations by LC–MS/MS analysis. The number of identified peptides of each protein is shown. (**B**) Flag-tagged plasmids encoding hRpn13 and its deletion mutants depicted in the left panel were transfected into HEK293T cells. The cell lysates were immunoprecipitated with anti-Flag antibody, followed by immunoblotting for hα6, UCH37, hRpn1, and Flag (right panel). (**C**) Schematic representation of the structures of wild-type UCH37 (FL) and KEKE domain deletion mutant (left panel). HEK293T cells stably expressing Flag-tagged UCH37 (FL), ΔKE, and an empty vector were lysed and subjected to immunoprecipitation with anti-Flag antibody, followed by immunoblot for Flag, hα6, hRpn1, and hRpn13 (right panel). (**D**) The extracts of cells stably expressing Flag-UCH37 and Flag-UCH37ΔKE were fractionated by 10–40% glycerol gradient centrifugation. Immunoblot analysis was performed for each fraction using antibodies against Flag and hRpn13. Asterisks indicate artifact bands. (**E**) GST pull-down analysis of recombinant proteins. GST, GST-UCH37, or GST-ΔKEKE were incubated with 6xHis-Rpn13 and precipitated as in Figure 3C, followed by silver staining.

Next, we examined the role of the KEKE motif of UCH37. As shown in Figure 5C, UCH37 that lacked the KEKE motif (UCH37ΔKE) did not associate with hRpn13 and other proteasome subunits, whereas full-length UCH37 did. Glycerol-density gradient analysis of the extracts showed that a large portion of full-length UCH37 co-sedimented with 26S proteasomes, whereas UCH37ΔKE was observed exclusively in much lighter fractions, presumably as a free form, and that overexpression of UCH37ΔKE did not affect the association of hRpn13 with 26S proteasomes (Figure 5D). In *in vitro* experiments, GST-UCH37 pulled down hRpn13, but GST-UCH37ΔKE did not (Figure 5E), verifying the results depicted in Figure 5C and D. These results indicate that the KEKE motif of UCH37 is necessary for interaction with hRpn13, and hence, with 26S proteasomes.

Knockdown of hRpn13 causes loss of UCH37 proteins

Next, we examined the relationship between hRpn13 and UCH37 in knockdown experiments. We also performed knockdown of USP14, a human ortholog of yeast Ubp6, which is another proteasome-associated DUB (Leggett *et al*, 2002), to examine the relative contributions of UCH37 and USP14 in deubiquitinating activities of 26S proteasomes. Intriguingly, knockdown of hRpn13 caused marked reduction of total cellular UCH37 proteins but not USP14 proteins. On the other hand, knockdown of UCH37 did not affect the level of hRpn13 proteins (Figure 6A). The observed phenotypes of UCH37 knockdown were similar to those of hRpn13 knockdown with regard to cell growth and levels of polyubiquitinated proteins, which were almost the same as the control (Figure 6B and C). Glycerol-density gradient analysis of the extracts of hRpn13-knockdown cells again showed loss of UCH37 proteins in both free and 26S proteasome fractions, with unchanged distributions of proteasome subunits such as hRpn1 and α6 (Figure 6D). Next, we examined the mechanism of decrease in UCH37 proteins in hRpn13-knockdown cells. Control and hRpn13-knockdown cells were treated with various protease inhibitors such as epoxomycin, which is highly specific for proteasomes, MG132, which inhibits both proteasomes and lysosomal enzymes, and E-64d and pepstatin A, which are specific to lysosomal cathepsins. Although these agents worked effectively in inhibiting the relevant proteases (as monitored by the accumulation of polyubiquitinated proteins for proteasome inhibition and accumulation of lipid-conjugated forms of LC3 proteins for inhibition of lysosomal enzymes; Komatsu *et al*, 2005), UCH37 was not increased by any of the inhibitors (Figure 6E). Pulse–chase experiments using HEK293T cells that stably expressed Flag-tagged UCH37 showed almost the same half-life of UCH37 proteins in knockdown cells and control cells (Figure 6F). Semiquantitative reverse transcription–polymerase chain reaction (RT–PCR) showed almost the same expression levels of UCH37 mRNA in hRpn13-knockdown cells and control cells (Figure 6G). Considered together, these results indicate that hRpn13 is required for maintaining normal protein levels of UCH37, and that loss of UCH37 proteins in hRpn13 is not due to metabolic instability of UCH37 proteins or due to repression of transcription of UCH37 mRNA. At present, the mechanism is not clear.

Knockdown of hRpn13 decreases deubiquitinating activities of 26S proteasomes

Finally, we tested the deubiquitinating activities of knockdown cells shown in Figure 6A. As there are abundant DUBs that are not associated with proteasomes, we partially purified complexes of 26S proteasomes and proteasome-associated DUBs by glycerol-density gradient centrifugation, and the 26S proteasome fractions identified by Suc-LLVY-MCA-hydrolyzing activities were used in the following experiments. As shown in Figure 7A, the 26S proteasome fraction of each knockdown cell contained proteasome subunits at a comparable level to each other. Proteins of hRpn13, UCH37, and USP14 were almost completely lost in 26S proteasomes of the cells transfected with siRNAs against hRpn13, UCH37, and USP14, respectively. The deubiquitinating activities of these samples were assayed using ubiquitin-AMC as a substrate. Notably, the deubiquitinating activities of hRpn13- and UCH37-deficient proteasomes were approximately only one-third of those of the control. In contrast, knockdown of USP14 did not significantly reduce the activity. Concomitant knockdown of USP14 with knockdown of hRpn13 or UCH37 did not have additive effects. These results clearly indicate that UCH37 is the dominant DUB associated with mammalian 26S proteasomes and that recruitment of UCH37 by hRpn13 is required for this activity.

Discussion

Adrm1 was originally described as a heavily glycosylated membrane protein of molecular mass 110 kDa (Shimada *et al*, 1991). However, recent studies showed that Adrm1 was hardly, if any, glycosylated and most of it could be detected as a 42 kDa protein (Simins *et al*, 1999; Hasegawa *et al*, 2001; Lamerant and Kieda, 2005). Likewise, the antibody against Adrm1 we raised in this report did not detect the 110 kDa form of Adrm1. Moreover, immunocytochemical analysis of HeLa cells using this antibody indicated that Adrm1 is a soluble protein distributed both in the cytosol and nucleus, which is quite similar to the distribution of proteasomes, as revealed by staining for hRpn1 (Figure 1). Database search analysis suggested that Adrm1 is a human ortholog of yeast Rpn13 subunit. Indeed, Adrm1 was identified in the purified 26S proteasomes at nearly stoichiometric amount, and so we designated it hRpn13. While this manuscript was in preparation, Jorgensen *et al* (2006) reported Adrm1 as a novel proteasome-associated factor (Jorgensen *et al*, 2006). We also identified hRpn2 as an hRpn13-interacting subunit (Figure 3). A previous report mapped the location of p37A (*Drosophila* ortholog of UCH37) in *Drosophila* 26S proteasomes to the interface between the base and the lid, by electron microscopy using gold-labeled ubiquitin-aldehyde bound to the p37A/UCH37 (Holzl *et al*, 2000), which is consistent with our results.

However, immunodepletion analysis showed that not all the 26S proteasomes contain hRpn13 (Figure 2D). In this regard, it is better not to call hRpn13 a subunit of proteasomes but rather regard it as one of the PIPs. Even in yeast, there is no definite evidence to indicate that Rpn13 is a constitutive subunit of proteasomes. In a quantitative mass spectrometric analysis of budding yeast 26S proteasomes, Rpn13 was identified by much smaller number of peptides, compared to authentic proteasome subunits (Guerrero *et al*,

2006). The relatively low homology between Adrm1 and yeast Rpn13 may reflect this fact, as genuine proteasome subunits, but not PIPs, have much higher similarities between human and yeast subunits. Knockdown experiments further revealed that hRpn13 is not essential for proteolysis or viability of mammalian cells, whereas knockdown of hRpt2, a 19S ATPase subunit, was fatal (Figure 4). It is noteworthy that all subunits of RP, except Rpn9, Rpn10,

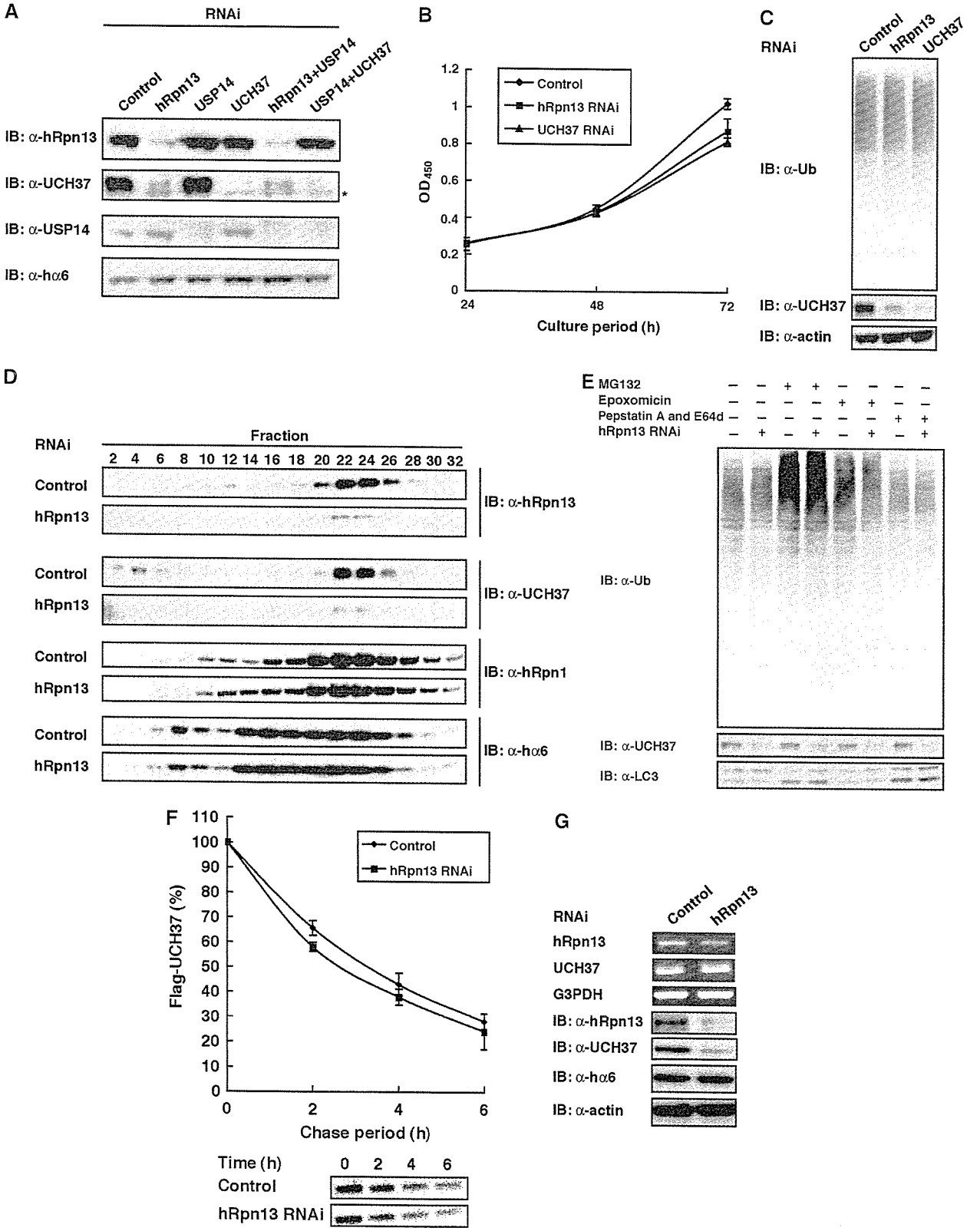

and Rpn15/Sem1, are essential for proliferation of the budding yeast examined so far. Considered together, these results suggest that hRpn13 plays an auxiliary role in the proteasome-dependent protein degradation.

hRpn13 has no known functional motifs and does not seem to be necessary for the structural integrity of proteasomes. Then, what is the role of hRpn13 in proteasomes? hRpn13 can be divided into three functional regions: the N-terminal, C-terminal, and the inserted regions. The former two regions are well conserved from budding yeast to human,

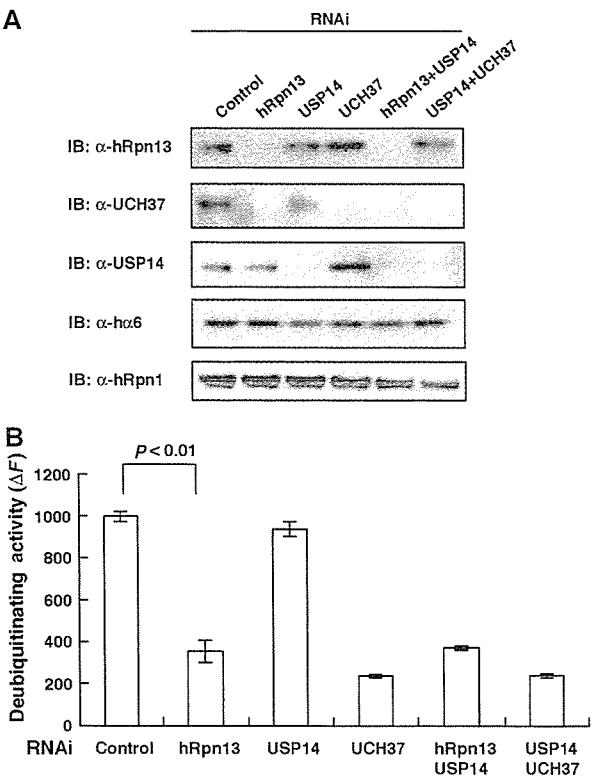

Figure 7 Knockdown of hRpn13 reduces deubiquitinating activities of 26S proteasomes. (**A**) hRpn13 and proteasome associating DUBs in knockdown cells. Cell extracts shown in Figure 6A were fractionated by 10–40% glycerol gradient centrifugation into 32 fractions. Immunoblot analysis of 26S proteasome fractions determined by Suc-LLVY-hydrolyzing activity was performed using the indicated antibodies. (**B**) The deubiquitinating activities of 26S proteasome fractions shown in panel A were measured using ubiquitin-AMC as a substrate. hRpn13- and UCH37-knockdown cells showed significantly reduced deubiquitinating activities ($P<0.01$). Data are mean±s.e.m. values of three independent experiments.

whereas the latter one is not found in budding yeast (Figure 1). We proved that the conserved N-terminal region is required for association with proteasomes (Figure 3). We also examined the biological role of the C-terminal region, and our results revealed that it serves as an acceptor for UCH37 (Figure 5). Moreover, loss of hRpn13 proteins caused concurrent loss of UCH37 proteins, indicating that hRpn13 recruits UCH37 to proteasomes and at the same time it is required for maintenance of UCH37 protein levels (Figure 6). As the half-life of UCH37 protein in hRpn13-knockdown cells was similar to that of control cell, the role of hRpn13 in maintaining UHC37 protein levels does not seem to be the stabilization of UCH37 protein. Consistent with this notion, neither the use of a proteasome inhibitor nor a lysosomal inhibitor resulted in accumulation of UCH37 proteins in knockdown cells. The amount of UCH37 mRNA was also unaltered in knockdown cells. At present, we do not know the reason for loss of UCH37 protein in knockdown cells, and the role of the insertion region is yet to be determined. No ortholog of UCH37 is found in budding yeast. Evolutionarily, UCH37 orthologs have emerged synchronously with the insertion region of Rpn13 orthologs. This region may have some role in the relationship with UCH37 and/or other proteins yet to be identified.

Ubp6 (USP14 in mammals) is another well-known DUB that associates with proteasomes. A mutation in USP14 in mice causes neurological disorders, demonstrating the importance of USP14 in mammals. Low expression of USP14 in mice is associated with reduced levels of free ubiquitin, suggesting its role in recycling ubiquitins (Anderson *et al*, 2005), as is also suggested in studies in budding yeast (Guterman and Glickman, 2004). However, the deubiquitinating activity of proteasomes is mainly attributed to UCH37 in fission yeast (Stone *et al*, 2004). Our present study also demonstrates that the deubiquitinating activities of 26S proteasomes are affected more profoundly by loss of UCH37 than USP14, indicating that UCH37 is the dominant DUB over USP14 in mammalian proteasomes. Recruitment of UCH37 by hRpn13 is essential for the activity of UCH37, as hRpn13 knockdown resulted in loss of UCH37, followed by a decrease in the deubiquitinating activity of 26S proteasomes at a level comparable to UCH37 knockdown. Further studies are required to distinguish the roles of USP14 (Ubp6) and UCH37 in organisms that have both molecules. It is plausible that the two molecules have distinct roles.

Despite the significant reduction of deubiquitinating activity of hRpn13-deficient proteasomes, they efficiently

Figure 6 Knockdown of hRpn13 causes loss of UCH37 proteins. (**A**) HEK293T cells were transfected with siRNA against hRpn13, UCH37, or USP14. Where indicated, cells were transfected with a mixture of siRNAs. After 96 h, cell extracts were subjected to SDS–PAGE, followed by immunoblotting with the indicated antibodies. (**B**) Growth rates of hRpn13 knockdown, UCH37 knockdown, and mock cells. The cells were seeded in triplicate in 96-well dishes on day 0 (72 h after transfection), cultured in normal growing medium, and their proliferation was measured every 24 h. Data are mean±s.d. values. (**C**) Cell extracts of hRpn13 knockdown, UCH37 knockdown, and mock cells were subjected to SDS–PAGE, followed by immunoblotting with the indicated antibodies. (**D**) Samples fractionated by 10–40% glycerol gradient centrifugation were immunoblotted with the indicated antibodies. (**E**) Lack of accumulation of UCH37 proteins in hRpn13-knockdown cells following inhibition of the proteasome or lysosomal cathepsins. HEK293T cells transfected with siRNA were treated with MG132 (50 μM, 2 h), epoxomycin (1 μM, 12 h), or E-64 and pepstatin A (10 μg/ml, 12 h). The cells were lysed and subjected to immunoblot. (**F**) Pulse–chase analysis of Flag-UCH37. HEK293T cells stably expressing Flag-UCH37 were pulse-labeled for 30 min with ^{35}S-labeled methionine and chased for the indicated time periods. After immunoprecipitation with M2 agarose, samples were separated by SDS–PAGE and autoradiographed (bottom panels). The upper panel shows the results of band quantitative analysis. Data are mean±s.d. values of three independent experiments. (**G**) hRpn13 knockdown does not alter UCH37 mRNA transcription. Semiquantitative RT–PCR (the upper three panels) and immunoblotting (the lower three panels) were performed using total RNA and proteins extracted from control and hRpn13-knockdown cells 48 h after transfection with siRNAs.

degraded substrate proteins such as ODC, ubiquitinated c-IAP, and IκBα (Figure 4). These observations seem to be in marked contrast to the case of yeast Rpn13, whose deletion caused a complete defect in degradation of a UFD substrate (Verma *et al*, 2000). However, as yeasts that lack Rpn13 are viable (Winzeler *et al*, 1999), the proteolytic defect is probably specific to UFD substrates. Rpn13 may recruit a component essential for degradation of UFD substrates in yeast. The precise role of hRpn13 and UCH37 still remains elusive. Curiously, knockdown of hRpn13 significantly increased the degrading activity of ODC but not that of ubiquitinated cIAP1 protein *in vitro* and IκBα *in vivo*. As sole knockdown of UCH37 did not increase the degrading activity of ODC (data not shown), the results observed in hRpn13 knockdown are not simply due to loss of UCH37. hRpn13 may influence access of protein to the channel of ATPase rings of proteasomes by sitting in the space between the base and lid (Holzl *et al*, 2000), or may recruit proteins that are relevant to proteolysis other than UCH37. At least from these results, both hRpn13 and UCH37 do not seem to be generally required for protein degradation by 26S proteasomes. It is assumed that UCH37 disassembles polyubiquitin chains from the distal end, shortening it such that the attached proteins can be released from the proteasome if there is a delay in efficient degradation (Stone *et al*, 2004). hRpn13 and UCH37 may be important in some specific situations. Further studies are required to determine the specific functions of hRpn13 and UCH37.

Materials and methods

Plasmids and cloning

The complementary DNAs (cDNAs) used in the present study were obtained by RT–PCR from total RNA isolated from HeLa cells or mouse livers using Superscript III (Invitrogen, San Diego, CA) and Pyrobest DNA polymerase (Takara Shuzo, Ohtsu, Japan). All amplified fragments were cloned into pcDNA3.1 vector (Invitrogen) and sequenced for confirmation. Deletion mutants (hRpn13ΔC, ΔN, N, ΔKE1 and ΔKE1 + 2, and UCH37ΔKE) were generated by PCR from wild-type hRpn13 and UCH37 and the Flag tag was introduced at the N-terminus of the constructs. For expression of GST and 6xHis fusion proteins, the cDNAs were subcloned into pGEX6P-1 (Amersham Life Science, Buckinghamshire, UK) and pET-28a (Novagen, Madison, WI) vector, respectively.

Immunological analysis

For immunoprecipitation analysis, HEK293T cells were transfected with plasmids using Fugene 6 (Roche, Mannheim, Germany). After 36 h, the cells were lysed with ice-cold phosphate-buffered saline (PBS) containing 1% Nonidet P-40 (NP-40) and centrifuged at 20 000 *g* for 10 min at 4°C. The supernatant was added with M2-agarose (Sigma Chemical Co., St Louis, MO) and rotated for 1 h at 4°C. The immunoprecipitates were washed five times with ice-cold PBS containing 0.5% NP-40 and then boiled in SDS sample buffer in the presence of β-mercaptoethanol (β-ME). Samples were subjected to SDS–PAGE, transferred to polyvinylidene fluoride membrane, and analyzed by immunoblotting with anti-Flag (M2; Sigma). Polyclonal antibodies against hRpn1, hRpn10, hRpt2, hRpn13, UCH37, and USP14 were raised in rabbits using recombinant proteins expressed in and purified from BL21RIL strain (Novagen) as GST fusion proteins: mouse Rpn1 (full length), mouse Rpn10 (residues 1–251), hRpt2 (residues 1–82), hRpn13 (residues 361–407), mouse UCH37 (residues 228–329), and human USP14 (full length). Anti-LC3 antibody was described previously (Komatsu *et al*, 2005). The antibodies for polyubiquitin and actin were purchased (FK2; MBL, Ina, Japan, Chemicon International Inc., Temecula, CA). All experimental protocols described in this study were approved by the Ethics Review Committee for Animal Experimentation of Tokyo Metropolitan Institute of Medical Science.

GST pull-down assay

Recombinant GST- or 6xHis-tagged proteins were produced in *Escherichia coli* and purified with glutathione Sepharose 4B (Amersham) or Ni-NTA Sepharose (Qiagen, Hilden, Germany). After elution of proteins from the beads, the preparations were dialyzed against buffer A (50 mM Tris–HCl (pH 7.5), 150 mM NaCl, 5 mM β-ME, and 10% glycerol). In GST pull-down analysis, 5 μg of each sample was mixed in 600 μl of buffer A and constantly rotated for 1 h at 4°C, and then 30 μl of glutathione Sepharose 4B was added and further rotated for 1 h. After washing with buffer A, bound proteins were eluted with 10 mM glutathione and subjected to SDS–PAGE, followed by immunoblot and silver staining (Wako Pure Chemical Industries, Osaka, Japan).

RNAi experiments

siRNAs targeting hRpt2, hRpn13, UCH37, and USP14 with the following 25-nucleotide sequences were purchased from Invitrogen: Rpt2, 5′-GGAGUACGAUGUGUAAGUGCCCAUU-3′; Rpn13, 5′-GGA GGGUCUACGUGCUGAAGUUCAAA-3′; UCH37, 5′-ACCGAGCTCAT TAAAGGATTCGGTT-3′; USP14, 5′-UCAGCAUCGUAACACCAGAA GAUAU-3′. siRNAs were transfected into HEK293T cells with Lipofectamine 2000 (Invitrogen) at a final concentration of 2 nM in six-well dishes. The cells were analyzed 96 h (hRpn13, UCH37, USP14, hRpn13 + USP14, and USP14 + UCH37) or 48 h (hRpt2) after transfection. For protease inhibition assay, HEK293T cells transfected with siRNA (96 h) were cultured in the presence or absence of protease inhibitors (50 μM MG132 for 2 h, 10 μg/ml E64d and 10 μg/ml pepstatin A for 12 h, or 1 μM epoxomycin for 12 h). Cell growth was measured using Cell Counting Kit-8 (Wako) according to the instructions provided by the manufacturer. Briefly, cells were seeded at 1×10^3 cells/well in 96-well plates. Absorbance was measured using Microplate reader (Bio-Rad).

Glycerol-density gradient analysis

Mouse livers were homogenized in a Potter-Elvehjem Homogenizer in buffer B (in mM, 25 Tris–HCl (pH 7.5), 2 ATP, 5 $MgCl_2$, and 1 dithiothreitol). HEK293T cells were lysed in buffer B containing 0.2% NP-40. The homogenates and lysates were clarified by centrifugation at 20 000 *g* and subjected to 10–40% (v/v) or 8–32% (v/v) linear glycerol-density density gradient centrifugation (22 h, 83 000 *g*) as described previously (Hirano *et al*, 2005).

In vitro assay of proteasome activity

Proteasome peptidase activity was measured using a peptide substrate, succinyl-Leu-Leu-Val-Tyr-7-amino-4-methyl-coumarin (Suc-LLVY-MCA), and the degradation of the recombinant ^{35}S-labeled ODC was assayed in the presence of ATP, an ATP-regenerating system, and AZ, as described previously (Hirano *et al*, 2005). For the assay of cIAP1 degradation, cDNAs encoding Flag-cIAP1 subcloned into pcDNA3.1 were transcribed *in vitro*, translated, and radiolabeled as described previously (Hirano *et al*, 2005). The ^{35}S-labeled Flag-cIAP1 was purified using M2-agarose (Sigma) and eluted with Flag-peptide (Sigma). For ubiquitination of cIAP1, 3 000 000 c.p.m. of ^{35}S-labeled cIAP1, 0.25 μg of E1, 0.9 μg of UbcH5, and 33 μg of ubiquitin (Sigma) were mixed and incubated in a volume of 80 μl for 90 min at 30°C, as described previously (Murata *et al*, 2001). Finally, 2.5 μl of the ubiquitination mixture was added to 10 μl of cell lysates in the presence of 2 mM ATP, incubated at 37°C for 20 min, and then radioactivities of trichloroacetic acid-soluble fractions were measured.

TNF-α-dependent IκBα degradation

HEK293T cells transfected with siRNA were treated with 100 μg/ml cycloheximide (Sigma) for 10 min, and then human TNF-α (Genzyme, Cambridge, MA) was added at a final concentration of 10 ng/ml. Changes in the protein levels of endogenous IκBα after treatment with TNF-α were analyzed by immunoblotting with anti-IκBα (c-21) (Santa Cruz Biotechnology, Santa Cruz, CA).

Deubiquitination assay

For ubiquitin-7-amino-4-methylcoumarin (ubiquitin-AMC) (Boston Biochem) hydrolysis assays, 10 μl of 26S proteasome fraction separated by glycerol gradient centrifugation was incubated with 0.25 μM ubiquitin-AMC for 15 min at 37°C. The release of AMC was measured fluorometrically.

Pulse–chase analysis

HEK293T cells stably expressing Flag-UCH37 were transfected with siRNA for hRpn13 or control siRNA. Pulse–chase experiments were performed as described previously (Hirano *et al*, 2005).

RT–PCR analysis

Total RNA (2.5 μg) was reverse transcribed using SuperScript III (Invitrogen) and oligo(dT)$_{20}$ primers. Specific primers for each gene were as follows: 5′-AAGGATCCATGAGCATCCTGGCCACG ATGAACG-3′ and 5′-TTCTCGAGTCAGTCCAGGCTCATGTCCTCC-3′ for hRpn13, 5′-AAGGATCCATGACGGGCAACGCCGGGGAG-3′ and 5′-TTCTCGAGTCATTTGGTTTCCTGAGCTTTC-3′ for UCH37, and 5′-ACCACAGTCCATGCCATCAC-3′ and 5′-TCCACCACCCTGTTGCT GTA-3′ for G3PDH.

Supplementary data

Supplementary data are available at *The EMBO Journal* Online (http://www.embojournal.org).

Acknowledgements

We thank Y Murakami for providing the ODC degradation assay system and K Furuyama for technical support. This work was supported in part by a grant to SM from JST and grants to SM and KT from the Ministry of Education, Science and Culture of Japan.

References

Anderson C, Crimmins S, Wilson JA, Korbel GA, Ploegh HL, Wilson SM (2005) Loss of Usp14 results in reduced levels of ubiquitin in ataxia mice. *J Neurochem* **95:** 724–731

Baumeister W, Walz J, Zuhl F, Seemuller E (1998) The proteasome: paradigm of a self-compartmentalizing protease. *Cell* **92:** 367–380

Coux O, Tanaka K, Goldberg AL (1996) Structure and functions of the 20S and 26S proteasomes. *Annu Rev Biochem* **65:** 801–847

Glickman MH, Ciechanover A (2002) The ubiquitin-proteasome proteolytic pathway: destruction for the sake of construction. *Physiol Rev* **82:** 373–428

Glickman MH, Rubin DM, Coux O, Wefes I, Pfeifer G, Cjeka Z, Baumeister W, Fried VA, Finley D (1998) A subcomplex of the proteasome regulatory particle required for ubiquitin-conjugate degradation and related to the COP9-signalosome and eIF3. *Cell* **94:** 615–623

Guerrero C, Tagwerker C, Kaiser P, Huang L (2006) An integrated mass spectrometry-based proteomic approach. *Mol Cell Proteomics* **5:** 366–378

Guterman A, Glickman MH (2004) Complementary roles for Rpn11 and Ubp6 in deubiquitination and proteolysis by the proteasome. *J Biol Chem* **279:** 1729–1738

Hasegawa K, Sakurai N, Kinoshita T (2001) Xoom is maternally stored and functions as a transmembrane protein for gastrulation movement in *Xenopus* embryos. *Dev Growth Differ* **43:** 25–31

Hirano Y, Hendil KB, Yashiroda H, Iemura S, Nagane R, Hioki Y, Natsume T, Tanaka K, Murata S (2005) A heterodimeric complex that promotes the assembly of mammalian 20S proteasomes. *Nature* **437:** 1381–1385

Holzl H, Kapelari B, Kellermann J, Seemuller E, Sumegi M, Udvardy A, Medalia O, Sperling J, Muller SA, Engel A, Baumeister W (2000) The regulatory complex of *Drosophila melanogaster* 26S proteasomes. Subunit composition and localization of a deubiquitylating enzyme. *J Cell Biol* **150:** 119–130

Ito T, Chiba T, Ozawa R, Yoshida M, Hattori M, Sakaki Y (2001) A comprehensive two-hybrid analysis to explore the yeast protein interactome. *Proc Natl Acad Sci USA* **98:** 4569–4574

Jorgensen JP, Lauridsen AM, Kristensen P, Dissing K, Johnsen AH, Hendil KB, Hartmann-Petersen R (2006) Adrm1, a putative adhesion regulating protein, is a novel proteasome-associated factor. *J Mol Biol* **360:** 1043–1052

Komatsu M, Waguri S, Ueno T, Iwata J, Murata S, Tanida I, Ezaki J, Mizushima N, Ohsumi Y, Uchiyama Y, Kominami E, Tanaka K, Chiba T (2005) Impairment of starvation-induced and constitutive autophagy in Atg7-deficient mice. *J Cell Biol* **169:** 425–434

Kumatori A, Tanaka K, Inamura N, Sone S, Ogura T, Matsumoto T, Tachikawa T, Shin S, Ichihara A (1990) Abnormally high expression of proteasomes in human leukemic cells. *Proc Natl Acad Sci USA* **87:** 7071–7075

Lam YA, Xu W, DeMartino GN, Cohen RE (1997) Editing of ubiquitin conjugates by an isopeptidase in the 26S proteasome. *Nature* **385:** 737–740

Lamerant N, Kieda C (2005) Adhesion properties of adhesion-regulating molecule 1 protein on endothelial cells. *FEBS J* **272:** 1833–1844

Leggett DS, Hanna J, Borodovsky A, Crosas B, Schmidt M, Baker RT, Walz T, Ploegh H, Finley D (2002) Multiple associated proteins regulate proteasome structure and function. *Mol Cell* **10:** 495–507

Li T, Duan W, Yang H, Lee MK, Bte Mustafa F, Lee BH, Teo TS (2001) Identification of two proteins, S14 and UIP1, that interact with UCH37. *FEBS Lett* **488:** 201–205

Li T, Naqvi NI, Yang H, Teo TS (2000) Identification of a 26S proteasome-associated UCH in fission yeast. *Biochem Biophys Res Commun* **272:** 270–275

MacArthur MW, Thornton JM (1991) Influence of proline residues on protein conformation. *J Mol Biol* **218:** 397–412

Murakami Y, Matsufuji S, Kameji T, Hayashi S, Igarashi K, Tamura T, Tanaka K, Ichihara A (1992) Ornithine decarboxylase is degraded by the 26S proteasome without ubiquitination. *Nature* **360:** 597–599

Murata S, Minami Y, Minami M, Chiba T, Tanaka K (2001) CHIP is a chaperone-dependent E3 ligase that ubiquitylates unfolded protein. *EMBO Rep* **2:** 1133–1138

Natsume T, Yamauchi Y, Nakayama H, Shinkawa T, Yanagida M, Takahashi N, Isobe T (2002) A direct nanoflow liquid chromatography-tandem mass spectrometry system for interaction proteomics. *Anal Chem* **74:** 4725–4733

Realini C, Rogers SW, Rechsteiner M (1994) KEKE motifs. Proposed roles in protein–protein association and presentation of peptides by MHC class I receptors. *FEBS Lett* **348:** 109–113

Shimada S, Ogawa M, Schlom J, Greiner JW (1991) Identification of a novel tumor-associated Mr 110 000 gene product in human gastric carcinoma cells that is immunologically related to carcinoembryonic antigen. *Cancer Res* **51:** 5694–5703

Shimada S, Ogawa M, Takahashi M, Schlom J, Greiner JW (1994) Molecular cloning and characterization of the complementary DNA of an M(r) 110 000 antigen expressed by human gastric carcinoma cells and upregulated by gamma-interferon. *Cancer Res* **54:** 3831–3836

Simins AB, Weighardt H, Weidner KM, Weidle UH, Holzmann B (1999) Functional cloning of ARM-1, an adhesion-regulating molecule upregulated in metastatic tumor cells. *Clin Exp Metast* **17:** 641–648

Smith DM, Kafri G, Cheng Y, Ng D, Walz T, Goldberg AL (2005) ATP binding to PAN or the 26S ATPases causes association with the 20S proteasome, gate opening, and translocation of unfolded proteins. *Mol Cell* **20:** 687–698

Stone M, Hartmann-Petersen R, Seeger M, Bech-Otschir D, Wallace M, Gordon C (2004) Uch2/Uch37 is the major deubiquitinating enzyme associated with the 26S proteasome in fission yeast. *J Mol Biol* **344:** 697–706

Suzuki H, Chiba T, Suzuki T, Fujita T, Ikenoue T, Omata M, Furuichi K, Shikama H, Tanaka K (2000) Homodimer of two F-box proteins βTrCP1 or βTrCP2 binds to IκBα for signal-dependent ubiquitination. *J Biol Chem* **275:** 2877–2884

Verma R, Aravind L, Oania R, McDonald WH, Yates III JR, Koonin EV, Deshaies RJ (2002) Role of Rpn11 metalloprotease in deubiquitination and degradation by the 26S proteasome. *Science* **298:** 611–615

Verma R, Chen S, Feldman R, Schieltz D, Yates J, Dohmen J, Deshaies RJ (2000) Proteasomal proteomics: identification of nucleotide-sensitive proteasome-interacting proteins by mass spectrometric analysis of affinity-purified proteasomes. *Mol Biol Cell* **11:** 3425–3439

Verma R, Oania R, Graumann J, Deshaies RJ (2004) Multiubiquitin chain receptors define a layer of substrate selectivity in the ubiquitin–proteasome system. *Cell* **118:** 99–110

Winzeler EA, Shoemaker DD, Astromoff A, Liang H, Anderson K, Andre B, Bangham R, Benito R, Boeke JD, Bussey H, Chu AM, Connelly C, Davis K, Dietrich F, Dow SW, El Bakkoury M, Foury F, Friend SH, Gentalen E, Giaever G, Hegemann JH, Jones T, Laub M, Liao H, Liebundguth N, Lockhart DJ, Lucau-Danila A, Lussier M, M'Rabet N, Menard P, Mittmann M, Pai C, Rebischung C, Revuelta JL, Riles L, Roberts CJ, Ross-MacDonald P, Scherens B, Snyder M, Sookhai-Mahadeo S, Storms RK, Veronneau S, Voet M, Volckaert G, Ward TR, Wysocki R, Yen GS, Yu K, Zimmermann K, Philippsen P, Johnston M, Davis RW (1999) Functional characterization of the *S. cerevisiae* genome by gene deletion and parallel analysis. *Science* **285:** 901–906

Yang Y, Fang S, Jensen JP, Weissman AM, Ashwell JD (2000) Ubiquitin protein ligase activity of IAPs and their degradation in proteasomes in response to apoptotic stimuli. *Science* **288:** 874–877

Yao T, Cohen RE (2002) A cryptic protease couples deubiquitination and degradation by the proteasome. *Nature* **419:** 403–407

Molecular Cell 24, 977–984, December 28, 2006 ©2006 Elsevier Inc. DOI 10.1016/j.molcel.2006.11.015

Cooperation of Multiple Chaperones Required for the Assembly of Mammalian 20S Proteasomes

Short Article

Yuko Hirano,[1] Hidemi Hayashi,[2,4] Shun-ichiro Iemura,[5] Klavs B. Hendil,[6] Shin-ichiro Niwa,[4] Toshihiko Kishimoto,[2,3] Masanori Kasahara,[7] Tohru Natsume,[5] Keiji Tanaka,[1] and Shigeo Murata[1,8,*]

[1]Laboratory of Frontier Science
Core Technology and Research Center
Tokyo Metropolitan Institute of Medical Science
Bunkyo-ku, Tokyo 113-8613

[2]Proteome Analysis Center

[3]Department of Biomolecular Science
Faculty of Science
Toho University
Funabashi, Chiba 274-8510

[4]Link Genomics, Inc.
Chuo-ku, Tokyo 103-0024

[5]National Institute of Advanced Industrial Science and Technology
Biological Information Research Center
Kohtoh-ku, Tokyo 135-0064
Japan

[6]Institute of Molecular Biology and Physiology
University of Copenhagen
13 Universitetsparken
DK 2100 Copenhagen
Denmark

[7]Department of Pathology
Hokkaido University Graduate School of Medicine
Sapporo, Hokkaido 060-8638

[8]PRESTO
Japan Science and Technology Agency
Kawaguchi, Saitama 332-0012
Japan

Summary

The 20S proteasome is a catalytic core of the 26S proteasome, a central enzyme in the degradation of ubiquitin-conjugated proteins. It is composed of 14 distinct gene products that form four stacked rings of seven subunits each, $\alpha_{1-7}\beta_{1-7}\beta_{1-7}\alpha_{1-7}$. It is reported that the biogenesis of mammalian 20S proteasomes is assisted by proteasome-specific chaperones, named PAC1, PAC2, and hUmp1, but the details are still unknown. Here, we report the identification of a chaperone, designated PAC3, as a component of α rings. Although it can intrinsically bind directly to both α and β subunits, PAC3 dissociates before the formation of half-proteasomes, a process coupled with the recruitment of β subunits and hUmp1. Knockdown of PAC3 impaired α ring formation. Further, PAC1/2/3 triple knockdown resulted in the accumulation of disorganized half-proteasomes that are incompetent for dimerization. Our results describe a cooperative system of multiple chaperones involved in the correct assembly of mammalian 20S proteasomes.

*Correspondence: smurata@rinshoken.or.jp

Introduction

The ubiquitin-proteasome system is the main nonlysosomal route for intracellular protein degradation in eukaryotes. Short-lived proteins as well as abnormal proteins are recognized by the ubiquitin system and are marked with ubiquitin chains as degradation signals. Polyubiquitinated proteins are then recognized and degraded by 26S proteasomes. The 26S proteasome is composed of one proteolytically active 20S proteasome and two 19S regulatory particles, each attached to one end of the 20S proteasome. The 20S proteasome is a barrel-shaped complex made of two outer α rings and two inner β rings that is a conserved architecture in eukaryotes (Groll et al., 1997, 2005; Unno et al., 2002). The α and β rings are each made up of seven structurally similar subunits, of the α or β type, respectively. The proteolytic activity is exerted by three of the β subunits, namely β1, β2, and β5, which are synthesized in an inactive precursor form and whose propeptides are removed to allow the formation of active sites, accompanied by the assembly of 20S proteasomes.

Our previous work indicated that the assembly of mammalian 20S proteasomes is an ordered multistep process, starting from α ring formation with the help of proteasome-specific chaperones named PAC1 (proteasome assembling chaperone 1) and PAC2 (Hirano et al., 2005). The PAC1-PAC2 heterodimer binds to early α subunit assembly intermediates that contain a restricted subset of α subunits and promotes the formation of heteroheptameric α rings. Moreover, PAC1-PAC2 is responsible for suppressing the formation of off-pathway, nonproductive α ring dimers and thus is important for efficient half-proteasome formation (Hirano et al., 2005). Mammalian half-proteasomes are composed of seven α subunits, seven β subunits, some of which are in precursor forms, and proteasome-dedicated chaperones such as hUmp1 (POMP, Proteassemblin, a homolog of yeast Ump1) (Burri et al., 2000; Griffin et al., 2000; Ramos et al., 1998; Witt et al., 2000) and PAC1-PAC2 (Hirano et al., 2005). Lastly, dimerization of the two half-proteasomes occurs with the help of hUmp1, which completes the maturation of 20S proteasomes, with removal of propeptides of β subunits followed by degradation of hUmp1 and the PAC1-PAC2 heterodimer (Chen and Hochstrasser, 1996; De et al., 2003; Heinemeyer et al., 2004; Hirano et al., 2005; Kingsbury et al., 2000; Nandi et al., 1997; Ramos et al., 1998; Schmidtke et al., 1996). However, the mechanism responsible for half-proteasome formation after the assembly of α rings, i.e., how β subunits and hUmp1 are assembled on α rings, remains elusive. We speculated that another chaperone might be involved in this step.

Results and Discussion

Identification of PAC3 as a Component of α Rings

To identify molecules that are potentially involved in 20S proteasome maturation, we purified α rings from HEK293T cells stably expressing Flag-PAC1 and analyzed them

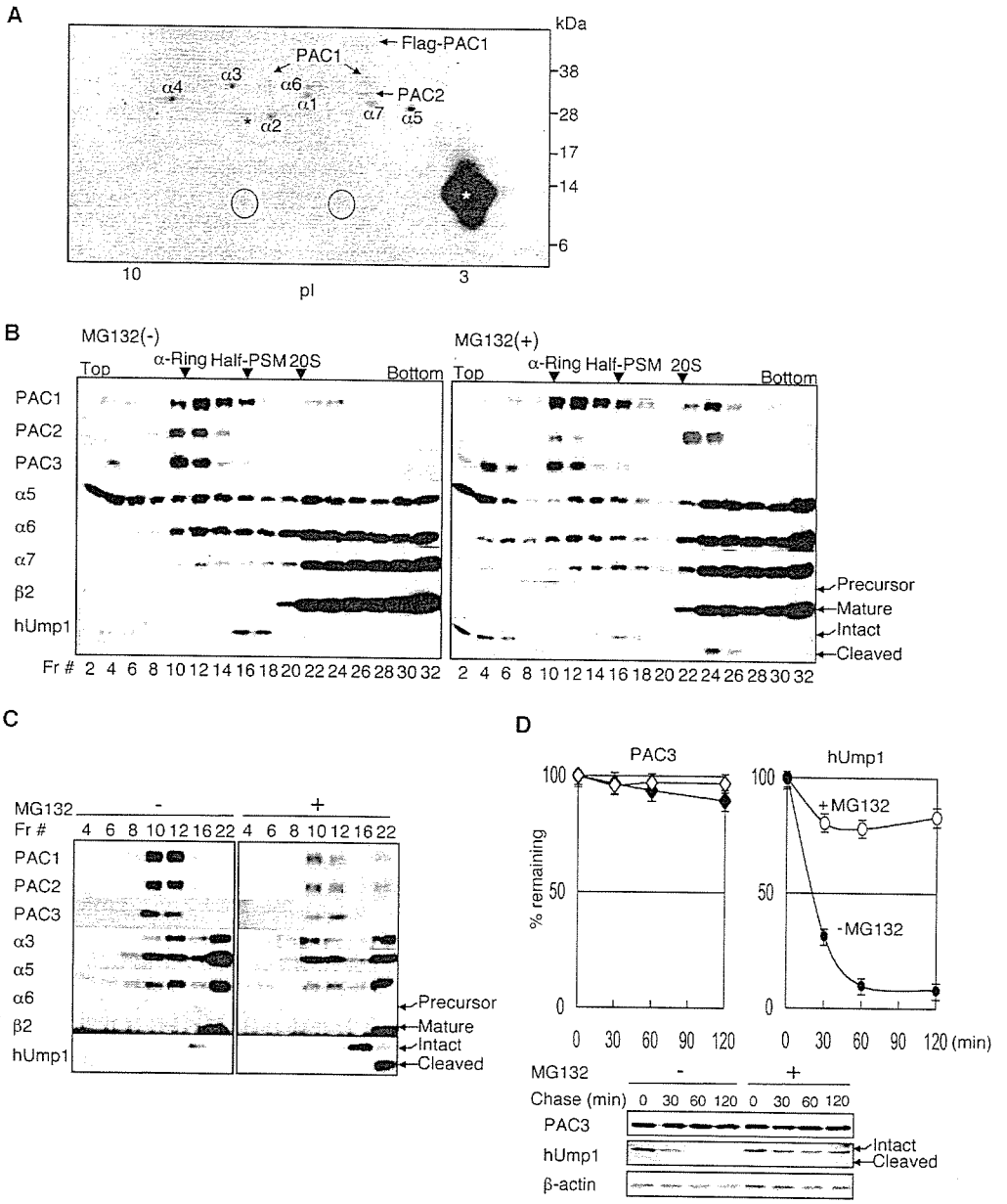

Figure 1. Identification of PAC3 as a Component of α Rings

(A) 2D-PAGE and CBB staining of purified α rings. The α rings were purified from HEK293T cells stably expressing Flag-PAC1 by glycerol gradient centrifugation followed by immunoprecipitation of α ring fractions with M2 agarose. All the spots were identified by MS/MS. The two spots indicated by circles represent hypothetical protein MGC10911. Asterisks indicate nonspecific spots.

(B) 4%–24% glycerol gradient centrifugation of the extracts of HEK293T cells treated with or without MG132. Fractions were immunoblotted as indicated. Arrowheads depict the locations of subcomplexes of proteasomes. Half-PSM, half-proteasomes; 20S, 20S proteasomes. Note that 26S proteasomes sediment near the bottom fraction.

(C) Fractions from (B) were immunoprecipitated with anti-α6 antibody, followed by immunoblotting.

(D) The half-life of PAC3 and hUmp1. Cycloheximide was added to HEK293T cells pretreated with or without 20 μM MG132 for 20 min, and the cells were chased for the indicated time points in the presence or absence of MG132, respectively. The cell lysates were subjected to immunoblotting for PAC3, hUmp1, and β-actin (loading control, bottom). The decay curves of PAC3 (top, left) and hUmp1 (top, right) were generated from the band quantification of the bottom panels. Data are mean ± SEM values of three independent experiments.

by two-dimensional polyacrylamide gel electrophoresis (2D-PAGE). In addition to the spots of α subunits and PAC1-PAC2 heterodimer, we found two spots of ~14 kDa. Using tandem mass spectrometry (MS/MS), we identified the two spots as a protein called MGC10911 (Figure 1A). We renamed it PAC3 (for proteasome assembling chaperone-3). PAC3 is a small protein of 122 amino acids with no distinct domains or homology to any other known proteins, and its function was entirely unknown. We found genes with significant similarity in metazoans, plants, and fungi, as for PAC2, PAC3, and hUmp1, but in metazoans and fungi as for PAC1 (Figure S1 in the Supplemental Data available with this article online).

First, to examine the behavior of endogenous PAC3, extracts from HEK293T cells were separated by glycerol

gradient centrifugation. PAC3 was located in the α ring fractions (fractions 10–12), i.e., in fractions without β subunits but with α subunits and PAC1-PAC2 (Figure 1B, left). The association of PAC3 with α subunits and PAC1-PAC2 was confirmed by immunoprecipitation with anti-α6 antibody followed by immunoblotting, indicating that PAC3 is a component of α rings, similar to PAC1-PAC2 (Figure 1C, left). Interestingly, when the cells were treated with a proteasome inhibitor, MG132, PAC3 was increased in the light fractions (fractions 2–6), whereas PAC1-PAC2 accumulated in the 20S proteasome fractions (fractions 22–24) as reported previously by our group (Figure 1B, right panels) (Hirano et al., 2005). This suggests that PAC3 dissociates from precursor proteasomes during the maturation pathway, unlike PAC1-PAC2 and hUmp1 (Hirano et al., 2005; Ramos et al., 1998). The increase in PAC3 in the light fractions does not represent an increase in newly synthesized PAC3 upon MG132 treatment, because PAC3 messenger RNA was not increased at this point of time (data not shown). To examine whether the stability of PAC3 is also regulated differently from that of PAC1-PAC2 and hUmp1, which have been shown to be short-lived proteins (Hirano et al., 2005; Ramos et al., 1998), we measured the half-life of PAC3 as well as that of hUmp1 by determining the protein levels at various time points after treatment with cycloheximide. As shown in Figure 1D, hUmp1 had a short half-life of about 20 min, which was greatly prolonged by MG132. This observation is consistent with the previous report (Ramos et al., 1998). As for hUmp1, we noted accumulation of its free forms (Figure 1B, right, fractions 2–6) as well as its cleaved forms in 20S proteasome fractions upon MG132 treatment (Figures 1B–1D). In contrast, PAC3 had a much longer half-life, which was not affected by MG132. These results suggest that PAC3 is involved in the maturation of 20S proteasomes and behaves differently from PAC1-PAC2 and hUmp1.

Knockdown of PAC3 Attenuates α Ring Formation

To elucidate the role of PAC3 in the assembly of the 20S proteasome in vivo, we performed small interfering RNA (siRNA)-mediated knockdown of PAC3 as well as PAC1+PAC2 (PAC1/2), PAC1+PAC2+PAC3 (PAC1/2/3), and hUmp1 to specify their distinct roles. In PAC3 knockdown cells, where we achieved a 75% reduction of PAC3 mRNA (data not shown), polyubiquitin-conjugated proteins accumulated to a level comparable to that in PAC1/2 knockdown cells (Figure 2A). In PAC1/2/3 knockdown cells, the accumulation of polyubiquitinated proteins was enhanced, and the effect of such knockdown was as large as with hUmp1 knockdown (Figure 2A). Consistent with these observations, the decrease in chymotrypsin-like activity of proteasomes was comparable between PAC3 and PAC1/2 knockdown, and the activity was profoundly reduced in PAC1/2/3 knockdown, similar to that in hUmp1 knockdown. These results suggest that PAC1-PAC2 and PAC3 are not epistatic with each other but rather work differently or compensate each other.

To determine the role of PAC3 in the assembly of 20S proteasomes, extracts of knockdown cells were subjected to glycerol gradient analysis (Figure 2C and Figure S2). To compare the quantity of relevant components in each fraction, fractions corresponding to α ring, half-proteasome, and 20S proteasomes in each knockdown experiment were electrophoresed in the same gel (Figure 2D). PAC1/2 knockdown resulted in reduction of α ring peak and emergence of α ring dimers in the half-proteasome fractions (fractions 14–16) as we reported previously (Hirano et al., 2005), and it turned out that PAC3 was a component of this abnormal structure (Figure 2C, bottom left, and Figure 2D, lane 7), indicating that PAC3 plays no role in inhibiting the formation of α ring dimers. The accumulation of PAC3 in light fractions (Figure 2C, bottom left, fractions 4–6) was probably due to ineffective α ring formation in PAC1/2 knockdown cells. Ectopic expression of PAC3 in PAC1/2 knockdown cells did not complement the phenotypes in regard to the formation of α ring dimers and reduction in proteasome activity (Figure S3), indicating that PAC3 and PAC1-PAC2 play distinct roles in α ring formation and do not function redundantly.

In PAC3 knockdown cells, we also observed a reduction of the α ring peak, but no α ring dimers (Figure 2C, top right). Consequently, half-proteasomes, which included α subunits, pro-β subunits, and hUmp1 in proportions like those observed in control cells, were formed to a lesser extent, resulting in decreased formation of 20S proteasomes (Figure 2D, lanes 8 and 13). In addition, PAC1-PAC2 accumulated in light fractions, and free forms of α subunits were increased in PAC3 knockdown cells as well as PAC1/2 and PAC1/2/3 knockdown cells (Figure 2C, top right, and Figure S4). These results suggest that PAC3 plays an important role in α ring assembly and that poor α ring formation resulted in surplus PAC1-PAC2 heterodimer and free α subunits in light fractions.

Simultaneous Loss of PAC1-PAC2 and PAC3 Causes Accumulation of Disorganized Half-Proteasomes

Intriguingly, in PAC1/2/3 knockdown cells, several α subunits and β subunits, including pro-β2 and hUmp1, cosedimented in the half-proteasome fractions to levels comparable to, or even higher (for example, hUmp1, pro-β1, and pro-β2) than, those in control cells, but still the formation of 20S proteasomes was severely impaired (Figure 2C, bottom right, and Figure 2D, lanes 9 and 14). Specifically, the amount of pro-β5, whose propeptide is essential for 20S proteasome formation in yeast (Chen and Hochstrasser, 1996), was much smaller in the complex observed in the half-proteasome fraction of PAC1/2/3 knockdown cells than control cells (Figure 2D, lanes 6 and 9, and Figure 2E). Considering that α ring formation is attenuated by knockdown of both PAC1/2 and PAC3, these results suggest that this complex of abnormal half-proteasomes, observed in PAC1/2/3 knockdown cells, accumulated because it could not dimerize to form mature 20S proteasomes, at least due to a shortage of pro-β5, which should accompany a disorganized constitution of this abnormal half-proteasomes.

Taken together, the knockdown experiments suggest that both PAC1-PAC2 and PAC3 contribute to α ring formation by separate mechanisms, and thus, the effects of knockdowns are additive. In addition, our results suggest that PAC1-PAC2 and PAC3 act cooperatively on the correct formation of half-proteasomes. On the other hand, knockdown of hUmp1 did not influence

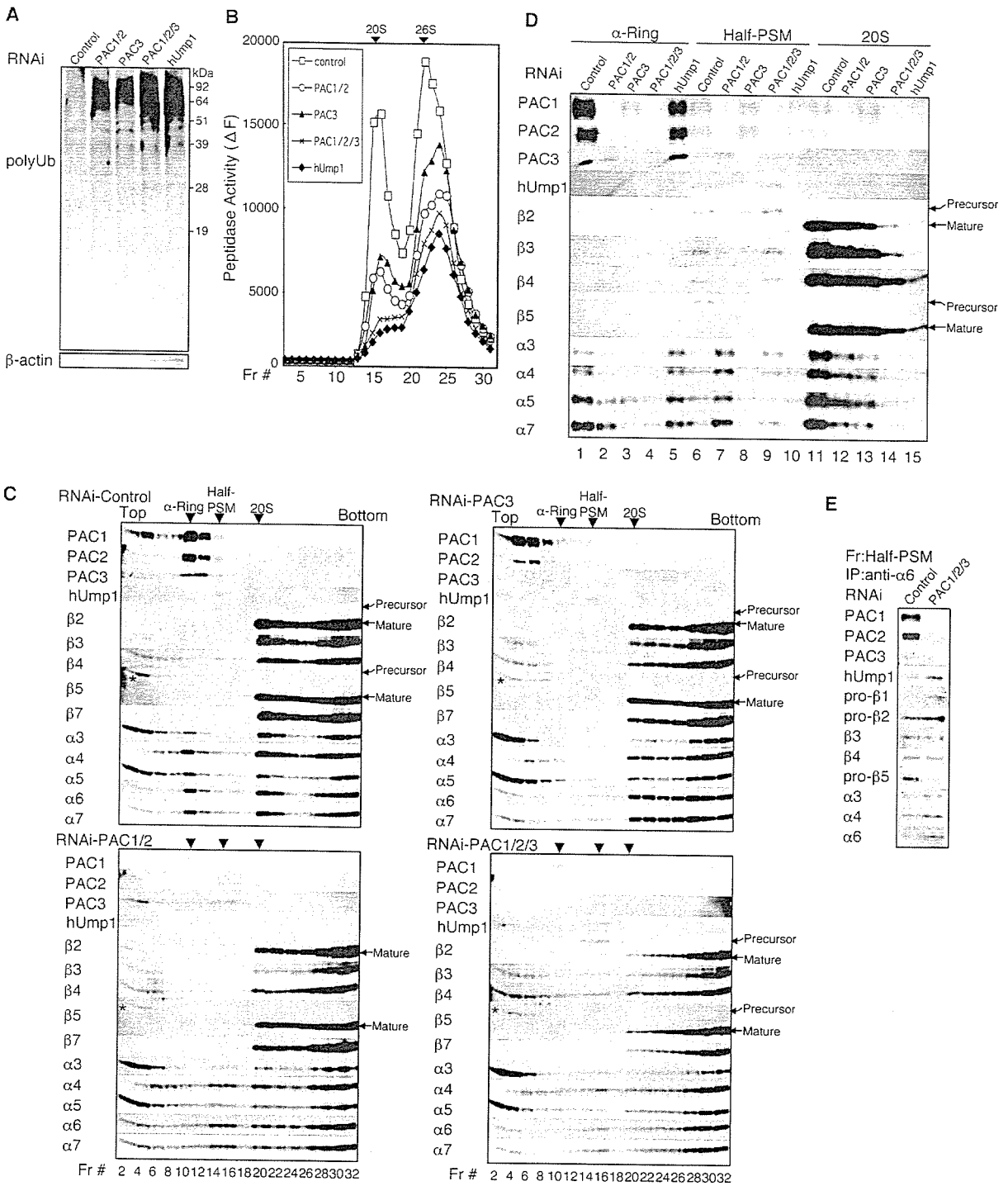

Figure 2. siRNA-Mediated Knockdown of PAC3 Causes Defect in Proteasome Assembly

siRNAs targeting PAC1/2, PAC3, PAC1/2/3, hUmp1, or control were transfected into HEK293T cells. The whole-cell extracts (A) and fractions separated by 8%–32% (B) or 4%–24% (C–E) glycerol gradient centrifugation were immunoblotted (A, C, D, and E) or assayed for Suc-LLVY-MCA hydrolyzing activity of proteasomes (B). In (D), the peak fractions of the indicated subcomplexes from (C) (α ring, fraction 12; Half-PSM, fraction 16; and 20S, fraction 22) were subjected to SDS-PAGE in the same gel to compare the quantity of subunits. (E) Fraction 16 of control or PAC1/2/3 knockdown cells from (C) was immunoprecipitated with anti-α6 antibody, followed by immunoblotting. Data are representative of four experiments.

the sedimentation pattern of PAC3 or PAC1-PAC2 (Figure S2), consistent with the notion that hUmp1 is involved in the last step of the assembly, i.e., dimerization of half-proteasomes, and not in α ring and half-proteasome formation (Hirano et al., 2005; Ramos et al., 1998).

PAC3 Directly Associates with Both α and β Subunits

To gain mechanistic insight into the action of PAC3 and the differences between PAC3 and PAC1-PAC2, we set up in vitro binding experiments. First, we examined direct interactions between PACs. PAC3 did not bind to

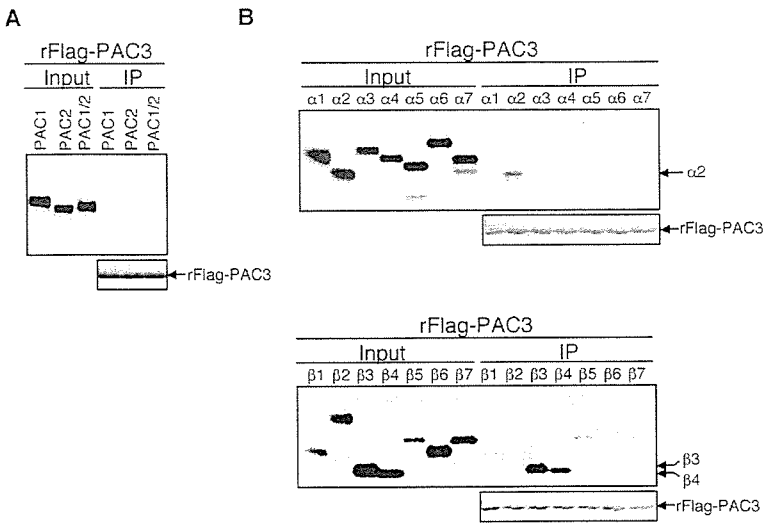

Figure 3. PAC3 Directly Binds to Both α2 and Several β Subunits

(A) Interactions of PAC3 with PAC1 and PAC2. Recombinant Flag-tagged PAC3 (rFlag-PAC3) was incubated with the indicated products translated and radiolabeled in reticulocyte lysates, immunoprecipitated with M2 agarose, and analyzed by SDS-PAGE and autoradiography.

(B) Interactions of PAC3 with individual α and β subunits. Interactions between rFlag-PAC3 and α or β subunits were analyzed as in (A).

PAC1 or PAC2 (Figure 3A). Next, we tested the interactions between PAC3 and each 20S proteasome subunit. PAC3 could directly bind to not only an α subunit (α2) but also to several β subunits, strongly to β3 and β4 but weakly to β1 and β5 (Figure 3B). This is in contrast to the property of PAC1-PAC2, which directly associated with α5 and α7, but not with any of the β subunits (Hirano et al., 2005). These results indicate that PAC1-PAC2 heterodimer and PAC3 are distinct entities that work at different aspects in the maturation of 20S proteasomes.

PAC3 Is Released from Precursor Proteasomes during Half-Proteasome Formation

Because PAC3 seemed to be released from precursor proteasomes during the maturation pathway (Figure 1B), we analyzed the precursor proteasomes that contain PAC3. An extract of HEK293T cells stably expressing Flag-PAC3, -hUmp1, or -PAC1 was separated by glycerol gradient centrifugation, and fractions 8–20, which included α rings (fraction 12) and half-proteasomes (fractions 16–18) were immunoprecipitated with anti-Flag antibody, followed by immunoblotting (Figure 4A). Flag-PAC3 did not precipitate hUmp1 or β subunits in half-proteasome fractions, and Flag-hUmp1 did not precipitate PAC3 at all (Figure 4A). Subsequently, we purified α rings and half-proteasomes from Flag-PAC2 and Flag-hUmp1 expressing cells, respectively, and subjected them to immunoblotting and CBB staining. Although half-proteasomes were loaded in much larger molar amounts, a band corresponding to PAC3, which was clearly visible in α rings, was not observed in half-proteasomes (Figure 4B and Figure S5). These results clearly show that the release of PAC3 from precursor proteasomes is coupled to the recruitment of hUmp1 and β subunits. Considering that PAC3 can directly bind to several β subunits in vitro (Figure 3B) and that PAC3 knockdown together with PAC1/2 knockdown resulted in production of disorganized half-proteasomes that were not competent for 20S proteasome formation (Figure 2), it is suggested that the association between PAC3 and β subunits is either intrinsically unstable in vivo or destabilized upon half-proteasome formation and that the release of PAC3 from precursor proteasomes is an obligatory step for the correct assembly of half-proteasomes by mediating interactions between α rings and β subunits.

Our present work provides a model (Figure 4C) where the chaperone PAC3 assists in the formation of α rings, together with PAC1-PAC2 heterodimer, and mediates correct formation of half-proteasomes in cooperation with PAC1-PAC2. PAC3 itself is then released and recycled in further rounds of proteasome assembly. The unique feature of PAC3 is its ability to interact with various β subunits, raising the possibility that it plays a role in the assembly of β subunits on α rings. In the present model, we emphasize that correct assembly of mammalian 20S proteasomes is achieved by the cooperative actions of multiple proteasome-specific chaperones.

Experimental Procedures

DNA Constructs

The cDNA encoding PAC3 was synthesized from total RNA isolated from HeLa cells using Superscript II (Invitrogen). PCR was carried out on the cDNA by using Phusion DNA polymerase (FINNZYMES). The cDNAs encoding PAC1, PAC2, PAC3, hUmp1, and proteasome α and β subunits were cloned into pcDNA3.1 (Invitrogen) and/or pIRESpuro3 (Clontech). All constructs were confirmed by sequencing. For expression of Flag-fusion protein, the cDNA was subcloned into pET22b (Novgen) in frame with a C-terminal Flag tag. For expression of GST and MBP-fusion proteins, the cDNAs were subcloned into pGEX6P-1 (Amersham) and pMAL (NEB), respectively.

Cell Culture

HEK293T cell lines were cultured in Dulbecco's modified Eagle's medium (Sigma), supplemented with 10% fetal calf serum (FCS), 100 IU/ml penicillin G, and 100 μg/ml streptomycin sulfate (all from Gibco-Invitrogen). Transfections of plasmids into HEK293T cells were performed with Fugene 6 (Roche). To generate stable cell lines, transfected HEK293T cells were selected with 5 μg/ml of puromycin. We used 20 μM MG132 (Peptide Institute) to inhibit proteasome activities for 2 hr before harvest. For cycloheximide-chase experiments, HEK293T cells were treated with 100 μg/ml cycloheximide (Sigma).

Protein Extracts, Immunological Analysis, and Antibodies

Cells were lysed in ice-cold lysis buffer (50 mM Tris-HCl [pH 7.5], 0.5% [v/v] NP-40, and 1 mM dithiothreitol [DTT]) with 2 mM ATP and 5 mM $MgCl_2$, and the extracts were clarified by centrifugation at 20,000 × g for 10 min at 4°C. The supernatants were mixed with

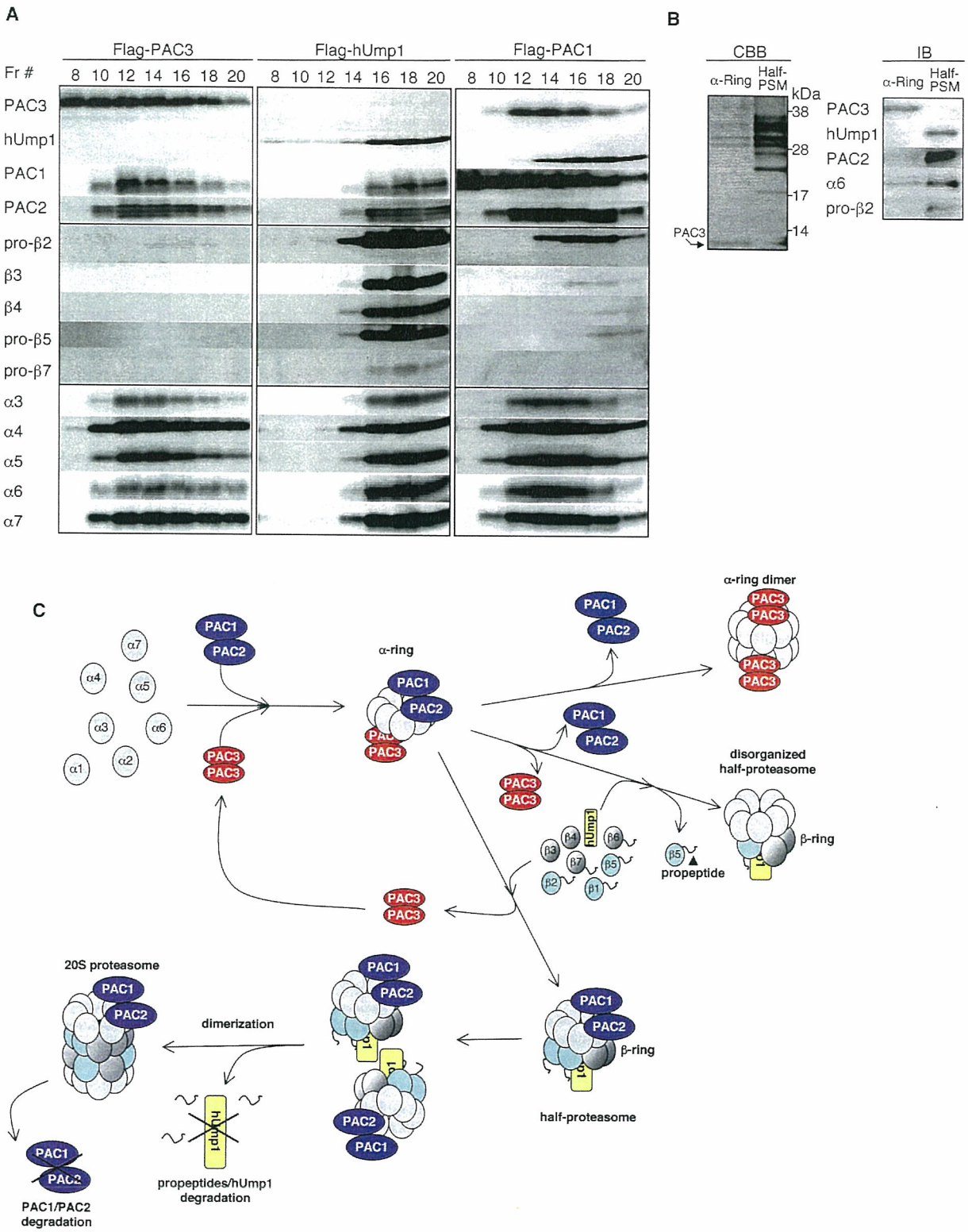

Figure 4. Mutually Exclusive Incorporation of PAC3 and hUmp1 into Precursor Proteasomes

(A) HEK293T cells stably expressing Flag-PAC3, -hUmp1, or -PAC1 were fractionated as in Figure 1B. The indicated fractions were immunoprecipitated with M2 agarose, resolved, and analyzed by SDS-PAGE and immunoblotting.

(B) SDS-PAGE followed by CBB staining (left) and immunoblotting (right) of purified α rings and half-proteasomes. α rings were purified from fraction 12 of Flag-PAC2 expressing cells. Half-proteasomes were purified from fraction 16 of Flag-hUmp1 expressing cells in (A). The band for PAC3 was identified by MS/MS. The 2D-PAGE analyses of these complexes are shown in Figure S5.

(C) A model for proteasome assembly assisted by multiple chaperones. PAC1-PAC2 heterodimer and PAC3, which probably forms homodimers based on the analysis of molecular sieve chromatography of the recombinant PAC3 (data not shown), assist α ring formation. Whereas PAC1-PAC2 suppresses off-pathway aggregation of α subunits and keeps α rings competent for half-proteasome formation, PAC3, which can bind

SDS sample buffer. SDS-PAGE (12% gel or 4%–12% gradient Bis-Tris gel [Invitrogen]) was performed according to the instructions provided by the manufacturer. The separated proteins were transferred onto polyvinylidene difluoride membrane and reacted with the indicated antibody. Development was performed with Western Lighting reagent (PerkinElmer). 2D-PAGE was performed as described previously (Murata et al., 2001).

For immunoprecipitation, we used antibodies MCP20 bound to protein G Sepharose (Amersham) in Figure 1C, antibodies MCP20 crosslinked to NHS-activated Sepharose (Amersham) in Figure 2E, or M2 Agarose (Sigma) in Figures 1A, 4A, and 4B. These beads were added to the extracts, mixed under constant rotation for 2 hr at 4°C, washed four times with lysis buffer with 30 mM NaCl, and boiled in SDS sample buffer. Otherwise, these washed samples were eluted with 100 μg/ml Flag peptides (Sigma) or with 0.2 M glycine-HCl (pH 2.8).

Anti-PAC1 and PAC2 polyclonal antibodies were described previously (Hirano et al., 2005). Anti-PAC3 polyclonal antibodies were raised in rabbits by using recombinant PAC3 (full-length) proteins, which were produced by cleavage of GST by PreScission protease (Amersham) after purification of GST-fused PAC3 proteins. Anti-hUmp1 polyclonal antibodies were raised in rabbits by using recombinant MBP-hUmp1 (full-length) proteins. Antibodies against proteasome α2 subunit (MCP21), α3 (MCP257), α4 (MCP34), α5 (MCP196), α6 (MCP20), α7 (MCP72), β1 (MCP421), β2 (MCP168), β3 (MCP102), and β7 (MCP205) were purchased from BioMol. Anti-β5 (P93250) and β4 (55F8) were prepared as described previously (Tanahashi et al., 2000). Anti-ubiquitin antibodies were obtained from Dako. Anti-β-actin antibodies were from Chemicon.

Glycerol Gradient Analysis

Cell extracts (1 mg of protein) were separated in 32 fractions by centrifugation (22 hr, 100,000 × g) in 4%–24% [v/v] or 8%–32% [v/v] linear gradients, as described previously (Hirano et al., 2005).

Binding Assay

In vitro labeling was performed by using TNT T7 Quick for PCR DNA system (Promega) with ^{35}S-labeled methionine, according to the procedure supplied by the manufacturer. Recombinant Flag-PAC3 proteins were expressed in *E. coli* and purified with M2 Agarose. Binding assay was performed in lysis buffer, and the resulting product was washed with lysis buffer with 150 mM NaCl before elution with Flag peptides. The eluates were separated by SDS-PAGE and visualized by autoradiography.

RNA Interference

siRNA targeting human PAC1, PAC2, PAC3, and hUmp1 with the following 19 nucleotide sequences were designed by B-Bridge and synthesized by Dharmacon. The targeting sequences of PAC1, PAC2, and hUmp1 were described previously (Hirano et al., 2005). These of PAC3 are 5′-CCGUGAAGGACAAAAGCAU-3′ and 5′-GAUCAAUUGUAGGAGGAAA-3′. Control siRNA (Non-specific Control Duplex VIII) was purchased from B-Bridge. Transfections of siRNAs into HEK293T cells were performed by using Lipofectamine 2000 at a final concentration of 50 nM. It was performed three times at intervals of 24 hr. The cells were analyzed 96 hr after first transfection.

Assay of Proteasome Activity

Peptidase activity was measured by using a fluorescent peptide substrate, succinyl-Leu-Leu-Val-Tyr-7-amido-4-methylcoumarin (Suc-LLVY-MCA), as described previously (Murata et al., 2001). Note that the assay was carried out in the presence of 0.03% SDS, which is a potent artificial activator of the latent 20S proteasome, as previously reported (Tanaka et al., 1989).

Supplemental Data

Supplemental Data include five figures and can be found with this article online at http://www.molecule.org/cgi/content/full/24/6/977/DC1/.

Acknowledgments

We thank K. Furuyama for technical support. This work was supported by grants from Japan Science and Technology Agency (to S.M.), the Ministry of Education, Science and Culture of Japan (to S.M. and K.T.), and NEDO (to T.N.). Y.H. was supported by Japan Society for the Promotion of Science.

Received: July 7, 2006
Revised: October 10, 2006
Accepted: November 15, 2006
Published: December 28, 2006

References

Burri, L., Hockendorff, J., Boehm, U., Klamp, T., Dohmen, R.J., and Levy, F. (2000). Identification and characterization of a mammalian protein interacting with 20S proteasome precursors. Proc. Natl. Acad. Sci. USA *97*, 10348–10353.

Chen, P., and Hochstrasser, M. (1996). Autocatalytic subunit processing couples active site formation in the 20S proteasome to completion of assembly. Cell *86*, 961–972.

De, M., Jayarapu, K., Elenich, L., Monaco, J.J., Colbert, R.A., and Griffin, T.A. (2003). β2 subunit propeptides influence cooperative proteasome assembly. J. Biol. Chem. *278*, 6153–6159.

Griffin, T.A., Slack, J.P., McCluskey, T.S., Monaco, J.J., and Colbert, R.A. (2000). Identification of proteassemblin, a mammalian homologue of the yeast protein, Ump1p, that is required for normal proteasome assembly. Mol. Cell Biol. Res. Commun. *3*, 212–217.

Groll, M., Ditzel, L., Lowe, J., Stock, D., Bochtler, M., Bartunik, H.D., and Huber, R. (1997). Structure of 20S proteasome from yeast at 2.4 Å resolution. Nature *386*, 463–471.

Groll, M., Bochtler, M., Brandstetter, H., Clausen, T., and Huber, R. (2005). Molecular machines for protein degradation. ChemBioChem *6*, 222–256.

Heinemeyer, W., Ramos, P.C., and Dohmen, R.J. (2004). The ultimate nanoscale mincer: assembly, structure and active sites of the 20S proteasome core. Cell. Mol. Life Sci. *61*, 1562–1578.

Hirano, Y., Hendil, K.B., Yashiroda, H., Iemura, S., Nagane, R., Hioki, Y., Natsume, T., Tanaka, K., and Murata, S. (2005). A heterodimeric complex that promotes the assembly of mammalian 20S proteasomes. Nature *437*, 1381–1385.

Kingsbury, D.J., Griffin, T.A., and Colbert, R.A. (2000). Novel propeptide function in 20 S proteasome assembly influences β subunit composition. J. Biol. Chem. *275*, 24156–24162.

Murata, S., Udono, H., Tanahashi, N., Hamada, N., Watanabe, K., Adachi, K., Yamano, T., Yui, K., Kobayashi, N., Kasahara, M., et al. (2001). Immunoproteasome assembly and antigen presentation in mice lacking both PA28α and PA28β. EMBO J. *20*, 5898–5907.

Nandi, D., Woodward, E., Ginsburg, D.B., and Monaco, J.J. (1997). Intermediates in the formation of mouse 20S proteasomes: implications for the assembly of precursor β subunits. EMBO J. *16*, 5363–5375.

Ramos, P.C., Hockendorff, J., Johnson, E.S., Varshavsky, A., and Dohmen, R.J. (1998). Ump1p is required for proper maturation of the 20S proteasome and becomes its substrate upon completion of the assembly. Cell *92*, 489–499.

Schmidtke, G., Kraft, R., Kostka, S., Henklein, P., Frommel, C., Lowe, J., Huber, R., Kloetzel, P.M., and Schmidt, M. (1996). Analysis of mammalian 20S proteasome biogenesis: the maturation of β-subunits is an ordered two-step mechanism involving autocatalysis. EMBO J. *15*, 6887–6898.

Tanahashi, N., Murakami, Y., Minami, Y., Shimbara, N., Hendil, K.B., and Tanaka, K. (2000). Hybrid proteasomes. Induction by interferon-γ and contribution to ATP-dependent proteolysis. J. Biol. Chem. *275*, 14336–14345.

directly to several β subunits, dissociates before the formation of half-proteasomes, a process coupled to the recruitment of β subunits and hUmp1. Loss of both PAC1-PAC2 and PAC3 before β subunit incorporation causes formation of disorganized half-proteasomes that lack pro-β5 almost completely. Released PAC3 is recycled. Two half-proteasomes dimerize with the help of hUmp1, and propeptides of β subunits (β1, β2, β5, β6, and β7) were cleaved. hUmp1 and PAC1-PAC2 are subsequently degraded by the newly formed active 20S proteasomes.